BUCKLING OF COLUMNS
WITH
SPECIAL REFERENCE
TO
PLASTIC BUCKLING

A Dissertation
Submitted in partial fulfilmentof the
requirements for the degree of
MASTER OF ENGINEERING
in
MECHANICAL ENGINEERING
(MACHINE DESIGN)

By

DALJIT SINGH BEDI

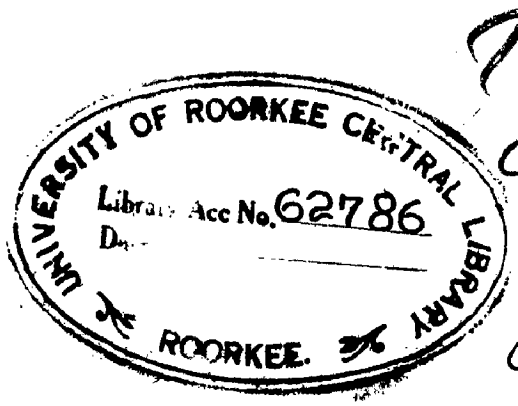

DEPARTMENT OF MECHANICAL ENGINEERING
UNIVERSITY OF ROORKEE
ROORKEE

1963

C_E_R_T_I_F_I_C_A_T_E

Certified that the dissertation entitled "Buckling of columns with special reference to plastic buckling" which is being submitted by Mr. Daljit Singh Bedi in partial fulfilment for the award of the Degree of Master of Engg. in Mechanical Machine Design of University of Roorkee is a record of students' own work carried out by him under my supervision and guidance. The matter embodied in this dissertation has not been submitted for the award of any other Degree or Diploma.

This is further to certify that he has worked for a period of 3½ months from 5th May, 1963 to 21st August, '63 for preparing dissertation for Master of Engineering Degree at the University.

Jainti Pd

Dated: August 21, '63.

(Jainti Prasad)
Lect. in Mech. Engg.
University of Roorkee,
Roorkee, U.P.

ACKNOWLEDGEMENTS

I wish to express my sincerest sense of gratitude to Prof. H.H Alvord, Visiting Professor of Mechanical Machine Design at the University of Roorkee; and Prof. L.B. Mankani, Reader in Mechanical Engineering, University of Roorkee, for suggesting the problem and giving valuable suggestions and comments at all stages of its progress.

My deep sense of gratitude goes to Prof. Jainti Prasad, Lecturer in Mechanical Engineering, University of Roorkee, for his valuable comments, instructions and guidance throughout the course of this study. His untiring enthusiasm was a constant source of inspiration to me due to which this work has assumed the present shape.

I will be failing in my duty if I do not express my sincerest gratitude to Prof. M.V. Kamlani, Head of the Mechanical Engineering Department, University of Roorkee for his patronizing guidance for the experimental work undertaken for this study.

My thanks are also due to M/S Goetze (India) Private Ltd., Bahadurgarh,(Patiala), for their help rendered to me by making available full Laboratory facilities for chemical analysis of various steels and Al-Mg-alloys used in the present work.

In the end I will like to thank Mr. Talwar, Laboratory Assistant, Material Testing Laboratory, Mr. K.B. Gaddi, Foreman Machine shop and other workshop staff for their co-operation in carrying out this experimental work.

D. B. BEDI

SYNOPSIS

The study in hand constitutes of tracing out the historical resume in development of the "Theories of Buckling with special reference to Plastic Buckling". Here in this work an attempt has been made to correlate the observed buckling load and stresses with those calculated by the various plastic buckling theories by plotting the curves of buckling stress Vs slenderness ratio for different materials, with various sections and various end conditions.

The effect of end-restraints on the working stress of a column has also been studied and inference drawn that the effects of end-restraints tend to be negligible and whatsoever is left should be dealt with by selecting the fixity coefficient with conservatism.

CONTENTS

LIST OF TABLES

1. INTRODUCTION

The maximum load that a member can take without failing to perform its function may be limited by the permissible elastic strain or deflection of the member, but elastic deflection which may constitute damage to a member can occur under the following different conditions:

(a) Deflection under conditions of static equilibrium such as the extension of a tension member, the angle of twist of a shaft and the deflection of a beam particularly under gradually applied load.

(b) The other structural action in which elastic deflection may limit the maximum load that can be applied to the member without causing the member to fail structurally is denoted as "Elastic Buckling". Buckling or the sudden deflection is associated with unstable equilibrium which causes the total collapse of the member. In buckling, the elastic deflections and stresses in the member are not proportional to the loads as buckling takes place, even though the material acts elastically i.e., stress is proportional to strain.

Elastic buckling arises out of the condition of neutral equilibrium that develops when applied load on the member reaches a so-called critical value. At this critical load the member is in equilibrium throughout a considerable range of small elastic deflections. But if the load is increased slightly above the critical value the deflection of the member increases abruptly and then it is not proportional to the load. And even in case the member is not

extremely slender, it will pass into a completely unstable condition due to inelastic action created by large deflections. This unstable condition will lead to total collapse.

This critical load or the buckling load is generally estimated by the well known Euler's Equation which gives critical load as

$$P_E = \frac{\pi^2 EI}{(L_e)^2}$$

$$\text{or} \quad P_E = \frac{\pi^2 EA}{(L_e/K)^2}$$

Where P_E = Euler's buckling load

E = Young's modulus of the material of column.

I = Least value of the second moment of area.

L_e* = Equivalent hinged length of the column and has different values for different end conditions.

A = Area of cross-section of column.

K = Least value of the radium of gyration of the section of column = $\sqrt{I/A}$.

L_e/K = Equivalent hinged slenderness ratio of the column.

At this critical load, the failure takes place purely due to the instability of the column and not due to excessive compressive stress. The compressive stress at this critical load can be written as $\sigma_c = P_E/A = E/(L_e/K)^2$

---

* $L_e = L$, the length of column for both ends hinged.

$L_e = L/2$, for both ends fixed.

$L_e = 2L$, for one end fixed and other free.

$L_e = L/\sqrt{2}$, for one end fixed and other guided.

As the equivalent slenderness ratio (L_e/K) of the column decreases the value of the compressive stress increases and for the relatively small slenderness ratio the direct compressive stress in the column attains the elastic limit in compression of the material before the buckling load. Thus the buckling of the column takes place when the direct stress is in the plastic region and it is known as the "Plastic Buckling". The Euler's expression is no more true for such columns and various theories have been put forward to determine the buckling load in the plastic region.

Here in this work an attempt has been made to correlate the observed plastic buckling loads and stresses with those calculated by the various plastic buckling theories by plotting the curves of buckling stress Vs slenderness ratio.

.....

2. TABLE OF UNITS AND SYMBOLS:-

P_E = Euler's buckling load; lbs.

E = Young's modulus of material; lb/in.^{2}

I = Least second moment of area; (in)^4

L = Length of the column; in.

L_e = Equivalent hinged length of column; in.

L_1 = Distance between ball centres of the pinned-end fixture; in.

K = Least value of the radius of gyration of the cross-section; in.

A = Area of cross-section of the column; (in.)^2

E_t = Tangent modulus; lb/in.^{2}

E_d = Double modulus or reduced modulus; lb/in.^{2}

ε = Strain; in./in.

σ = Stress; lb/in.^{2} or K.S.i.

σ_{cr} = Observed cripling stress; lb/in.^{2} or K.S.i.

σ_E = Euler's cripling stress; lb/in.^{2} or K.S.i.

σ_t = Engesser's stress or calculated cripling stress on the basis of tangent modulus theory; lb/in.^{2} or K.S.i.

σ_d = Calculated cripling stress on the basis of double modulus theory; lb/in.^{2} or K.S.i.

K.S.i. = Kilo pound per sq.in.

= 1000 lb/in.^{2}

d = Dia. of test specimen.

.....

3. REVIEW OF LITERATURE:

3.1. Theories of Buckling.

The buckling load for a column is taken to be the axial load that will hold the column in a slightly deflected position, and, since an ideal column would not bend under any axial load, a small lateral force must be applied to produce the initial deflection. This procedure, however, may be carried out in either of the two ways: (a) The lateral force may be assumed to be applied first and then the axial load required to hold the column in the slightly bent position is applied and the lateral force removed; or (b) The unknown buckling critical load may be assumed to be applied first and then the lateral force is applied to cause the deflection, and is then removed. For elastic behaviour of the column the solution for the buckling load will be the same for the two procedures, since the physical process constitutes a reversible system and hence does not depend on the strain history in arriving at a given physical state. Thus for the columns whose slenderness ratio is such that the nominal stress is within the compressive elastic limit of the material at buckling load, the Euler's equation for buckling load of columns, namely

$$P_E = \frac{\pi^2 EI}{(L_e)^2} \qquad \ldots\ldots\ldots\ldots(1)$$

$$\text{or} \quad \sigma_E = \frac{\pi^2 E}{(L_e/K)^2} \qquad \ldots\ldots\ldots\ldots(2)$$

has long been accepted.

But, if the physical process is non reversible, such as occurs in inelastic behaviour of material, the order of

applying the forces to the column in the two procedures would lead to different values for the buckling loads. The main condition involved in the process may be emphasized by stating that, for inelastic behaviour, a single-valued relationship between stress and strain does not exist. But in addition it may be pointed out that a single-valued relationship between stress and strain will exist not only for elastic strains but also for inelastic strains provided that all strains increase as the load increases i.e., no fibre in the member is allowed to unload.

The two solutions for the buckling load, therefore, will be for the assumptions, (a) that the lateral force and the last increment of the axial load are applied simultaneously so that the strains in all the fibres at any cross-section increase although they are not uniformly distributed on the section after the lateral force is applied, and (b) that an axial load equal to the buckling load is applied first and then followed by the application of a small lateral force which deflects the column; the bending in this case causes the strains in the fibres on the convex side to decrease and on the concave side to increase.

The essential difference in the two assumptions lies in the fact that under the second assumption the strains in some of the fibres on the convex side behave elastically and hence the change in stress $\Delta\sigma$ accompanying the decrease in strain $\Delta\varepsilon$ is given by $\Delta\sigma = E\Delta\varepsilon$, in which E is the Young's modulus of elasticity, whereas under the first

assumption $\Delta\sigma = E_t \Delta\varepsilon$ for each fibre, in which E_t is the tangent modulus corresponding to the inelastic stress σ ($\sigma = P/A$ where P is buckling load).

Based on the first assumption in 1889 Engesser[1] suggested the tangent modulus theory in which he pointed out to replace the Young's modulus E, in the equation No.1 for buckling load, by tangent modulus E_t is given by

$$E_t = \frac{d\sigma}{d\varepsilon} \qquad \ldots\ldots\ldots\ldots(3)$$

It is the local slope of the stress-strain diagram. Euler's equation modified in this manner becomes

$$\sigma_t = \frac{\pi^2 E_t}{(L_e/K)^2} \qquad \ldots\ldots\ldots\ldots(4)$$

This is referred to as the tangent-modulus formula or the Euler-Engesser formula. The buckling stress, σ_t, determined by this theory is called the Engesser stress or the tangent-modulus-stress.

After the appearance of Engesser's original paper in 1889, the tangent-modulus-theory was criticised on the grounds that it did not take into account the fact that during buckling a portion of the cross-section would be subjected to a decreasing stress, for which the elastic modulus would apply. This led to the development of the double-modulus theory[1], in which an effective or 'Reduced modulus' or 'Double modulus', E_d was determined based on the second assumption as mentioned above. The buckling stress or double modulus stress is given by replacing the Young's modulus, E,

---

(1) See Reference 1.

by double modulus E_d in the Euler's formula

$$\text{i.e., } \sigma_d = \frac{\pi^2 E_d}{(L_e/K)^2} \quad \ldots\ldots\ldots\ldots(5)$$

and the value of E_d [2] was calculated as

$$E_d = \frac{4E_t}{\left(1+\sqrt{\frac{E_t}{E}}\right)^2} \quad \ldots\ldots\ldots\ldots(6)$$

The double modulus theory was considered to be the correct theory of inelastic column action until 1946 when F.R.Shanley [3] showed that it represented a paradox. In order to exceed the Engesser-buckling stress, it was necessary that the column remains straight until that stress is reached and the effective modulus be greated than E_t. But a real column will not remain straight or will not wait to bend until the double-modulus buckling stress, σ_d, is reached as is assumed in the derivation of the double-modulus formula. In fact, even when great care is exercised in testing a real column, there is sufficient deviation from ideal conditions to cause the column to start to deflect laterally at a direct stress that is even less than σ_t, the tangent-modulus stress. But such small lateral deflections are accompanied by increments of strain $\Delta\varepsilon$ sufficiently small to nearly justify the conditions assumed in the derivation of the tangent-modulus formula, namely, that the stress increment $\Delta\sigma$ accompanying the bending strain increment $\Delta\varepsilon$ shall be given by the expression $\Delta\sigma = E_t\Delta\varepsilon$. If however an attempt is

---

(2) - See Reference 2. pp 599-602.

(3) - See Reference 3.

made to increase the direct stress above σ_t, it will be found that except for materials having a constant value of E_t a real column will not permit the direct stress to reach the value σ_d as given by the double-modulus formula; the column will buckle and collapse at a stress less than σ_d.

During plastic buckling the increase in the buckling stress beyond the Euler-Engesser value given by equation No.4, will depend on the variation of the tangent modulus with the increasing stress. In highly curved region of the stress-strain diagram, which is sometimes known as Knee, the tangent modulus drops very rapidly with increasing stress (Fig.15 & 16; 17 & 18 and also formaterials of indefinite Y.P); consequently very little increase in Euler-Engesser-stress would be obtained. In the so called plastic range, beyond the Knee of the diagram the tangent modulus has a relatively low value and does not change rapidly with increasing strain. The maximum column-buckling stress will therefore approach the value predicted by the double-modulus-theory, which permits a relatively large increase in buckling stress for low values of E_t/E.

The foregoing remarks which apply only to columns made of materials exhibiting a compressive stress-strain curve of gradual curvature above the proportional limit, (such as for Al alloys, heat treated special ferrous alloys etc.) and experiencing small strains may be interpreted that:

"The inelastic buckling stress for a real column that deviates very little from ideal conditions is predicted satisfactorily by the tangent modulus formula, and the

reduced-modulus formula only gives the upper limiting value of the plastic -buckling-stress that cannot be expected to be attained in a real column [2].

For the materials having a definite yield point(such as Mild Steel) , the slope of the compressive stress-strain curve changes abruptly to zero when the elastic limit is reached; the stress-strain curve suddenly becomes horizontal and remains so until, relatively large inelastic strains have developed. A column having a relatively small slenderness ratio and made of such material would buckle when the stress in the column reaches the elastic limit (yield point) in compression of the material; in other words, plastic behaviour is not accompanied by an increase in stress as is found to occur for materials not having a yield point (e.g. Al alloy). The so-called flat top stress-strain diagram means that the stress in the column remains constant at the elastic limit until the plastic compressive strains attain a value equal to the full length of the flat or horizontal position of the curve. This, in turn, means that before such a large plastic strain could be developed, the deviations from ideal conditions, even though very small would permit bending to start, leading

---

See-Reference 2. pp 606.

its buckling. From the above discussion it is clear that for an ideal column in the plastic range:

1. Engesser stress represents the maximum[2] stress for which the column has only one equilibrium configuration. Upto this stress the idealised column must remain straight; beyond this stress it may bend.

2. The double-modulus stress represents the upper limit for the stress that can theoretically be reached as the column continues to bend with increasing stress. To develop the double-modulus stress, it would require infinite lateral deflection at a constant[4,5] value of tangent-modulus which is impossible.

3. For a given column of a particular material, the maximum stress that can be developed will generally be only slightly greater[6] than the Engesser stress, because of the rapid decrease in E_t with increasing stress. Therefore the Engesser stress is considered as the practical upper limit for column strength.

3.2. Effects of End-Restraint:

In theory and restraint has a very simple effect; It merely changes the effective column length. In practice, however, the accurate determination of the effects of end-restraint for any column except a pin-ended column is a difficult problem.

---

(4) See Ref.4, (5) See Ref. 5.

(2) See Ref.2 pp 604-605 ; (6) See Ref.6.

The long standing conception of a fixity coefficient as a multiplying factor has perhaps given rise to an exaggerated idea of the effects of end restraint.

Mr. Von Karman[7] and others had shown that the fixity coefficient $\sqrt{C}$ can be used as a multiplying factor, but only for elastic case (Euler's formula). According to Vou Karman for elastic range buckling

$$L_{eff} = L/\sqrt{C} \qquad \ldots\ldots\ldots\ldots\ldots(7)$$

Where L_{eff} = Effective length of column

L = Actual length of column

$\sqrt{C}$ = Fixity coefficient *

In the plastic range the values of C given in the footnote may not be true but in general the equation (7) will hold good. After lot of experiments it was estimated by Vou Karman that end-restraint causes a marked increase in buckling strength only for long slender columns and not for short ones. The efficiently designed (i.e., allowable stress approaching the yield point) structures cannot be made proportionally stronger by increasing the amount of end restraint. In other words the effect of end restraint on column strength in the plastic range is very small. For example in aircraft structures, the compression members are designed to develope ultimate stresses that approach the

---

(7) See Ref. (7)

* C=1 for both ends pinned

C=4 for both ends fixed

C=$\frac{1}{4}$ for one end fixed and other free

C=2 for one end fixed and other guided.

compressive yield stress.

.....

4. DISCUSSION.

4.1. APPARATUS USED IN EXPERIMENT.

(i) Amsler's Universal testing machine of maximum capacity of 20 tons with 4 different load ranges of 2,5,10 and 20 tons.

(ii) Specially designed fixtures for loading of columns for pinned ends and fixed ends conditions to suit the above machine.

(a) The fixture for the fixed ends consists of two Mild Steel blocks as shown in figure No.1, upper one to be fitted in the fixed head of the machine. It was kept push-fit in the machine head so that proper concentricity may be maintained. Similarly the lower block was kept on the moving bed of the machine and the clearance between the two was push-fit. Both the blocks were case hardened upto about 40C rockwell hardness No.In the upper end lower blocks blend holes* of $0.4395^{**}_{0.4375}$ in diameter, to a length of 3/16" on each side, were drilled

---

* It may be pointed out that firstly the test pieces for fixed end conditions were tested by placing within the plane flat ends of the machine and compressed as such, but due to the presence of no fixing moments at the ends the test pieces after and even prior to buckling bent down with definite slopes at the ends. Therefore to provide fixing moments at the ends they were kept within the blind-holes of the end blocks only with push-fit tolerances.

** The size of test-specimens is discussed further.

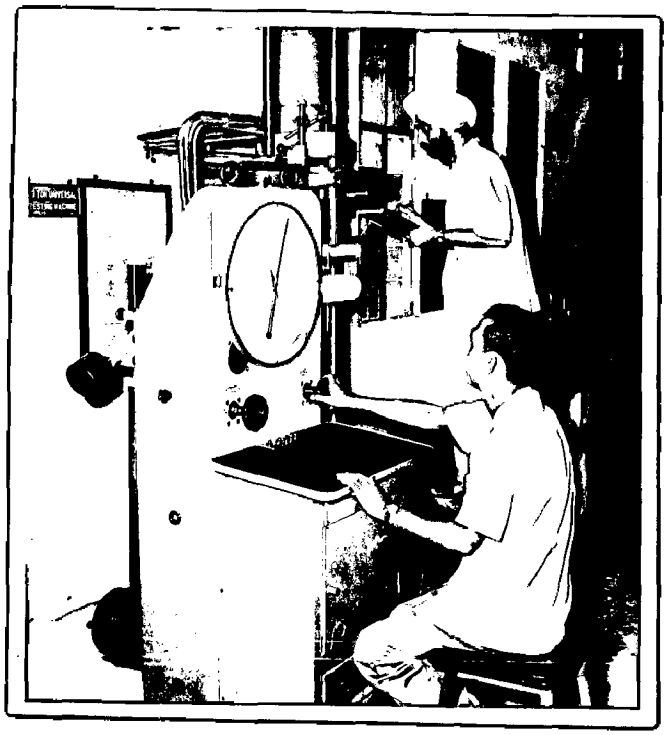

Compression test on M.S. specimen

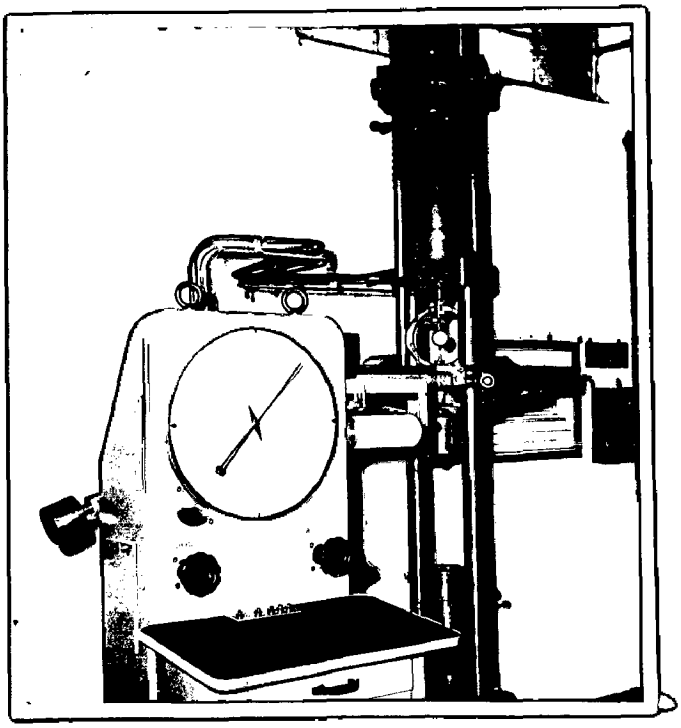

ibration of 5 ton Scale
Avsler's 20 ton Universal
ting machine

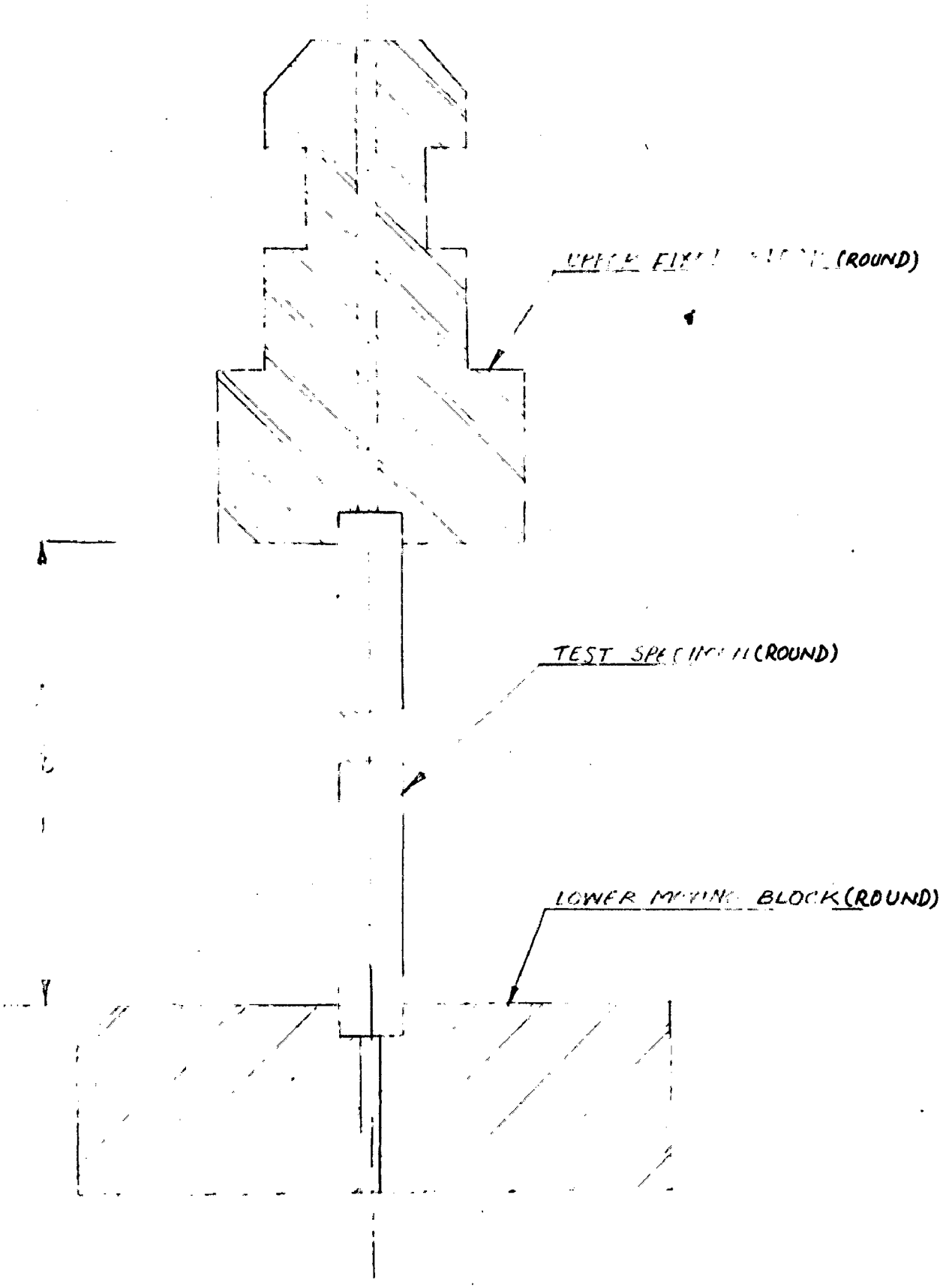

FIG. 1 FIXED-END FIXTURE

When the load is applied, initially the entire length of the test piece is compressed and due to the lateral expansion the ends of the test piece become rigidly fixed in the end blocks thereby fulfilling more or less the required fixed-end conditions. For the calculation purposes the length of the test piece which remains out of the blocks is taken into consideration. After failure of the test-specimen by buckling, it was taken out from the end blocks by hammering a 1/8" nail through the longitudinal holes provided in the blocks for this purpose.

(b) PINNED-END FIXTURE.

The assembly drawing of the pinned-end fixture is shown in figure No.2. It has got eight components as mentioned in Figure No.2. itself. The load is transmitted from the machine heads through "Upper Fixed Block-1" and "Lower moving block-8" to the hard steel Balls-7 ; then through the "Swivelling blocks-5" to the test specimen. All the components are of mild steel and were used after their proper case hardening upto 40-C Rockwell (specially the surface coming into contact of the balls). Two supporting pins-2 are screwed to the upper-fixed-block and two supporting rings-(3) are attached to the upper swivelling block by means of screws-4. The supporting rings-3 have sufficiently large diameters as compared to the supporting-pin-2 diameters so that any tilting of the upper swivelling block may be maintained without thereby giving any physical contact between the supporting pins and the supporting blocks. At the time of actual buckling there is every

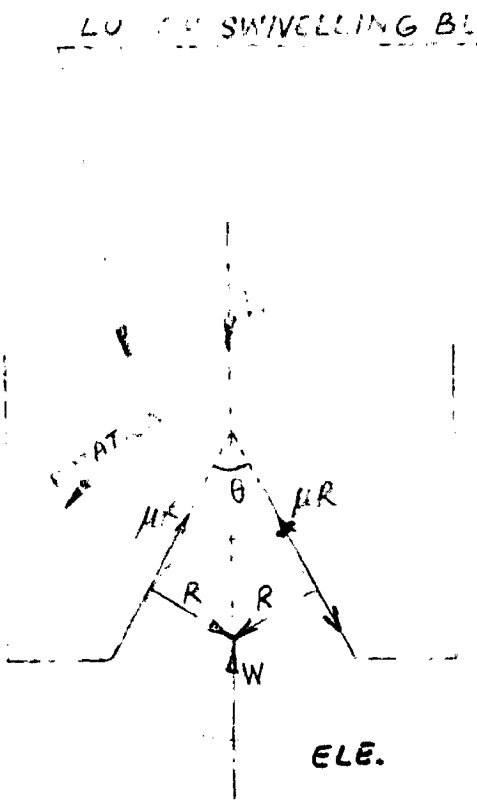

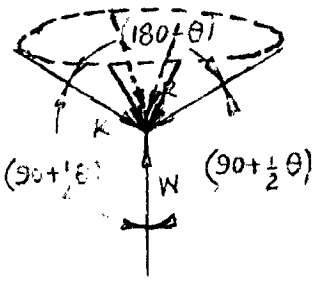

(i) BALL IN EQUILIBRIUM UNDER THE ACTION OF W, R & .

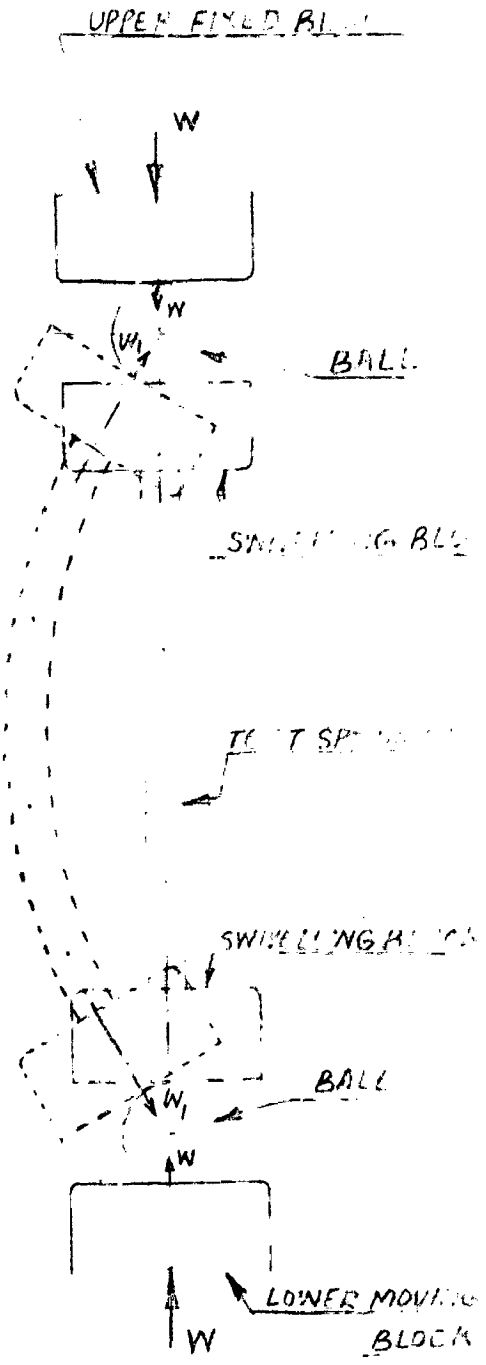

(ii) $\theta = 180°$
BALL SLIPS AWAY UNDER THE ACTION OF W & W1 WHEN THE SPECIMEN BENDS SLIGHTLY.

FIG-20:- MATHEMATICAL ANALYSIS OF CONE ANGLES.

possibility of falling of the upper swivelling block as well as the ball. To avoid this, the supporting rings and supporting pins have been provided. They will come in contact with each other and the swivelling block, with the ball on it, will hang through the rings on the pins.

The balls rest within the two conical cavities one in each of the swivelling blocks and the other in the upper-fixed block or the lower moving block. The mathematical aspect of the design of cone is shown below:-

The ball is in equilibrium under the action of load 'w' and reaction 'R' by the cone.

From figure 2a-(i)

$$W = R \sin\tfrac{1}{2}\theta$$

$$\text{i.e., } R = \frac{W}{\sin\tfrac{1}{2}\theta}$$

If F is the total frictional force obstructing the turning of cone over the ball or vice versa, then

$F = \mu R$ (where μ = Coefficient of friction.)

$$= \frac{\mu W}{\sin\tfrac{1}{2}\theta}$$

$$\text{i.e., } F = \frac{\mu W}{\sin\tfrac{1}{2}\theta}$$

Therefore to have least frictional effect $\sin\tfrac{1}{2}\theta$ should be as large as possible

i.e., $\tfrac{1}{2}\theta = 90^\circ$ or $\theta = 180^\circ$

But if $\theta = 180^\circ$, due to some manufacturing eccentricity there is every possibility of slip over of the swivelling

blocks and it will be very difficult to put the test piece on the machine for buckling with pinned ends. Secondly even if we are some how able to put the test specimen on to the machine and we start loading., then due to slight manufacturing eccentricity there will be introduced some bending/moment on the test specimen due to which it will start bending. This will introduce a condition of complete instability as is clear from the exaggerated position of test specimen with the swivelling blocks as shown dotted in figure 2a(ii). Under the action of two forces W & W_1 the balls will be forced to slip away and the fixture will cease to function. Thus if the cone apex angle approaches 180^0 the stability of the fixture will vanish. Therefore the stability requirements tend to reduce the apex angle to a value as low as possible depending upon the size of the ball. So a compromise between the two was tried. Here the most economical size of ball for 7/16" dia. Mild Steel test specimens will be $\frac{1}{2}$ in. dia of hardened high carbon steel. Accordingly the cone apex angle is kept at 120^0 so that the contact point with the ball is approximately near the middle of the cone surface. Moreover that way it is not very near the edge of central 1/8" dia. hole which will have to be drilled before the cone can be made by boring tool. On the opposite sides of the conical cavities in the swivelling blocks-5, concentric blind holes of 3/16 in. diameter, within $\pm$ 0.00025 in. tolerance of concentricity, were drilled to a depth of 5/16 in. so as to take up the test-specimen end-snugs of diameter $\begin{matrix}0.1873\\0.1870\end{matrix}$ in.

and length 3/16 in. By doing so, the placement of=the test specimen within the fixture is assured to be concentric with the load axis within 0.0015 in. maximum eccentricity on the final setting.

(c) STRAIN GAUGES AND BRIDGE AMPLIFIER.

(i) Rohit 120 ohms. S.R-4 strain gauges - 8 No.

(ii) Strain gauge D.C.Bridge amplifier.

(iii) Avometer.

(d) Micrometer of least count 1/10,000 inch and vernier callipers of 1/1000 inch accuracy were used to measure the diameters and lengths of the test specimens respectively.

(e) A Batty's dial gauge of ½ in. range and 1/10,000 in. accuracy, with a magnetic base was used to measure the contraction while obtaining the load-deformation (or stress-strain) curves of materials in compression.

(f) Two proving rings one each of 5 tons and 10 tons capacity to calibrate the 5 ton and 10 ton range scales of the Amsler's Universal testing machine.

4.2 EXPERIMENTAL PROCEDURE.

The sole purpose of the equipment was to measure the buckling load. As explained earlier the "Buckling"is identified, vaguely , by the abrupt bending of the column. But at the same time the practical column will definitely have some eccentricity and some initial curvature due to which, even though the column is loaded below the elastic-stress-load, the column will be deflected further, while simultaneously the load is being increased. This was confirmed with the help

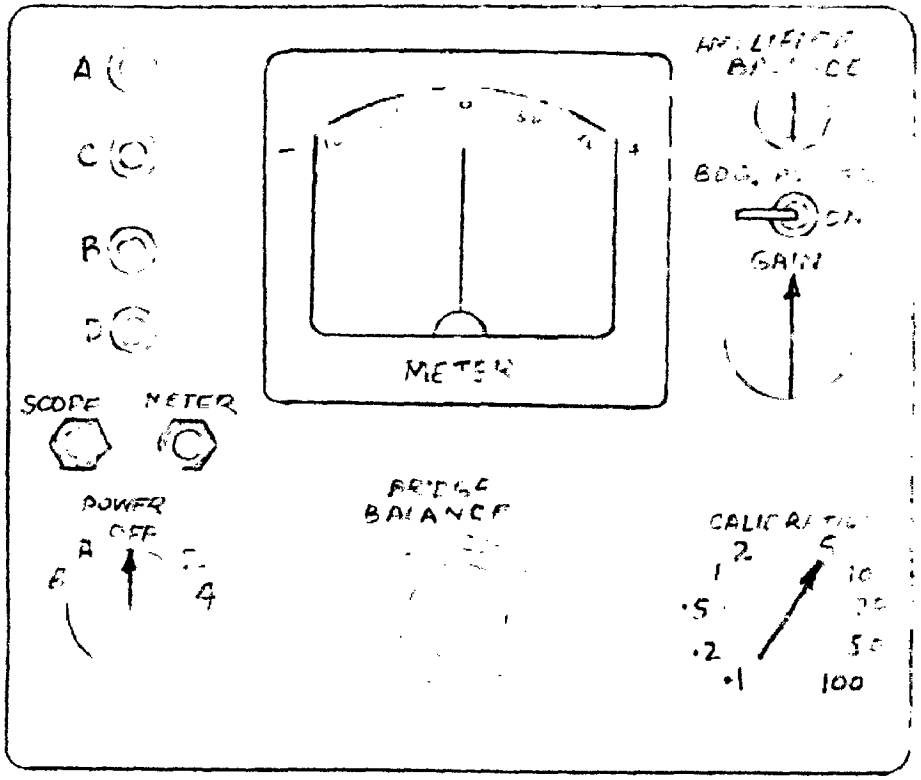

(i.)

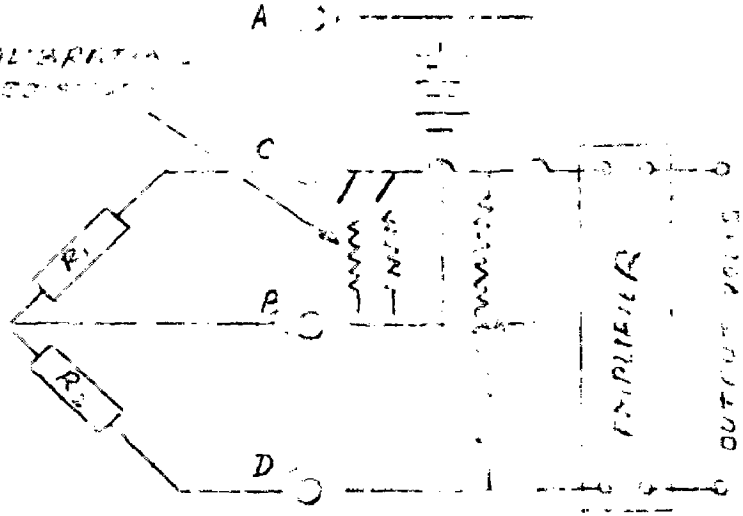

(c.)

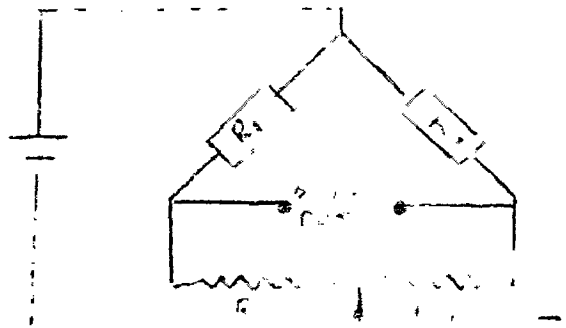

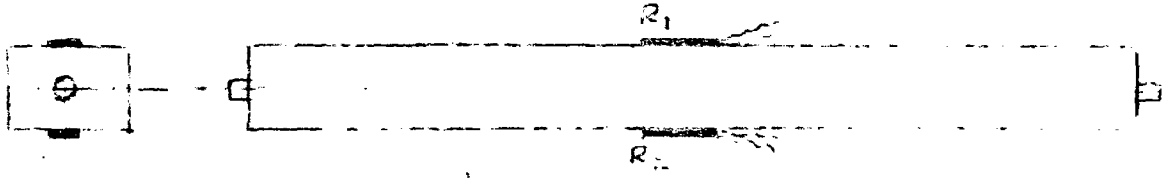

a. TEST PIECE WITH STRAIN GAUGES

b. D.C. BRIDGE AMPLIFIER

of strain gauges and D.C.Bridge amplifier as explained below:

Four test-specimens were selected at random two of Mild Steel rectangular section and two of Al-Mg-alloy nearly square section. On each of these test specimens two S.R-4 strain gauges taken from the same lot were cemented on the middle section of the test-specimens, the grid lengths being parallel to the length of the test piece, their planes being parallel to the neutral axis of the cross-section and each being placed on the opposite face of the piece in such a way that the planes of gauges are parallel to the axis having the least second moment of area of the section as is shown in figure No.3(a). The two gauges are connected to the D.C.Bridge amplifier (shown in figure 3b)* as per the circuit diagram shown in figure 3c* . The principle of this circuit diagram is 2-gauge Wheatstone's Bridge as illustrated in figure 3d.

Since gauges are in adjacent arms of the wheat-stone's bridge, the bridge output for the concentric test pieces will be zero as the two gauges are giving the strains of the same nature and being put in the adjacent arms of the bridge their effect is subtractive. But the moment buckling starts, because of the opposite nature of stresses on the convex and concave sides of the bent test specimen, the bridge will give net positive output thereby indicating the buckling point.

When the abovementioned test specimens were put to axial

---

* See Ref.8 pp 53.

compressive loading there was very little but gradual increase in the output voltage of the two gauge bridge circuit. Side by side the load deformation curve for the buckling specimen was being recorded on the automatic recorded mounted on the universal testing machine. It showed a gradual increase in load and corresponding increase in deformation.

As the load was increased further a point was reached when the column bent abruptly at a quicker rate even though the load pointer of the universal testing machine as well as automatic recorded showed an abrupt decrease in load. Thus the highest point on the load-deformation curve as obtained on the automatic recorder will correspond to the buckling load of the specimen under test. This was confirmed by the instantaneous deflection of the D.C.Bridge Amplifier-meter-needle to its maximum, when simultaneously the load pointer started showing an abrupt decrease in load.

Thus the experimental procedure was to record the load-deformation curve of each and every test specimen and the buckling load was read from this curve corresponding to the highest point of the curve. The rate of loading was kept the same for all the specimens by keeping the same valve opening.

In addition to the buckling loads compressive stress-strain diagrams for the different materials for which the buckling tests were performed, were obtained in order to determine the buckling loads (stresses) according to the existing tangent and reduced modulus theories. For this compressive test pieces of the same diameter as of the

columns and of lengths equal to twice the diameter were put to compression. As such the diameter was 7/16" and length 7/8 in. The deformation was measured with the help of dial gauge of accuracy 1/10,000 in. at the different compressive loads.

The calibration was done with the help of 5 ton and 10 ton proving rings with the calibration certificates provided with them.

Chemical analysis for different materials was done for determining the carbon percentage in Mild Steel and Mg. percentage in Al-Mg-alloy.

4.3. RANGE OF MEASUREMENT.

As mentioned above the main object of the experiment was to investigate the buckling stresses for different slenderness ratios, more particularly in the plastic range. One or two readings for each case were taken in the elastic range also so that we could ensure the change over point from elastic to plastic buckling.

The elastic limit of the Mild Steel out of round specimens is 48000 lb/in.^{2} or 48 K.S.i and Young's modulus is 29.4×10^6 p.s.i. (see next article). Therefore as pointed above the tests will be performed for a stress as low as 45000 lb/in^2. to ensure the change over point from elastic to plastic range of buckling. Now for the elastic range since Euler's equation is valid we have, for the fixed end conditions which will ask for greater lengths of the specimens,

$$\sigma_{\varepsilon} = \frac{4\pi^2 E}{(L/K)^2}$$

and for the extreme case σ_E = 45000 p.s.i.

we have $(\frac{L}{K})^2 = \frac{4\pi^2 \times 29.4 \times 10^6}{45000}$

or $\frac{L}{K} = 161$

But the maximum length that the machine could hold in compression was 22 inches

$\therefore$ for L = 22 in. K=22/161

and for round specimens K = D/4

$\therefore$ $D = \frac{4 \times 22}{161} \simeq 0.5$ in.

Hence the most appropriate diameter of the M.S.round specimens that could be tested in compression with the 20 ton Amsler's Universal testing machine was $\frac{1}{2}$ in. But from the manufacture point of view 7/16 in. nominal dia (or 0.4385 / 0.4375 in.dia) was kept which could be easily turned on lathe out of $\frac{1}{2}$ in. M.S.bar stock.

Thus for D = 7/16 in. K=D/4 = 7/64

$\therefore$ L = 7/64 x 161 = 17.6 in.

To allow for portions to go within fixture -

$$L = 17.6 + 0.375 \simeq 18"$$

On the other side to avoid buckling the length of the compression round-test-piece was kept twice the diameter. Thus a test piece of 7/16" dia and length 7/8" will not buckle and the corresponding slenderness ratio = 4L/D

$$= \frac{4 \times 7 \times 16}{8 \times 7} = 8$$

But for buckling the slenderness ratio was arbitrarily kept at 16 towards its least value. For this value of

slenderness ratio and dia = 7/16".

$$\text{Length } L = 16 \times \frac{D}{4} = 4 \times \frac{7}{16}$$

$$= 1\tfrac{3}{4}".$$

To allow for portions to go within fixture length of the shortest test specimen = $1\frac{3}{4} + \frac{3}{8} = 2\frac{1}{8}$ in.

Thus for the fixed end conditions the length of the round specimens of 7/16 in. dia. was having a range from $2\frac{1}{8}$ in. to 18 in. and the corresponding slenderness ratio range was 16 to 161 approximately. For the M.S. 7/16" dia. round specimens with pinned ends the slenderness ratio will evidently be half that for fixed-ends specimens for the same buckling stress range. Its range was kept from 16 to 90 approximately. The dia. of the pinned-end specimens was kept the same as for fixed end specimens so as to have the same size effect in the buckling of columns with different end conditions.

Now coming to the Al-Mg.alloy round specimens with fixed ends the diameter was kept the same as of M.S.specimens viz., 7/16 in. because the same fixture was used for loading purposes. And it follows that for the pinned end conditions also the diameter is kept the same as 7/16 in. As regards the slender-ness ratio range it was calculated in a similar fashion as for M.S.specimens. The range of slenderness ratio for fixed end specimens was 20.7 to 130 and for pinned ends 20.6 to 118.8.

As regards the section of the rectangular M.S.specimens it was kept $\frac{1}{2}$"x $\frac{3}{8}$" because the available stock with the stores was 5/8" square section bar and the most economical

rectangular section which can be cut out of the rolled bar on the milling machine is ½"x3/8". The slenderness ratio range was calculated in a similar fashion as for M.S.specimens. Range of slenderness ratio with pinned ends was 17.3 to 86.6.

As far as the square-sectioned Al-Mg-alloy test pieces were concerned, to have the maximum feasible length for the longest test piece, the cross-section was calculated as for M.S.specimens, to be 5/8"x5/8", which was made by milling out of ¾" square rolled bars. The slenderness ratio range was calculated in a similar manner as had been shown above for M.S.round specimens. Range was 18.6 to 82.2 for pinned ends.

As discussed above the following * were the ranges of slenderness ratios for various sets.

7/16 in.dia. M.S.specimens fixed ends	17.11 to 135.8.
7/16 in.dia. M.S.specimens Pinned ends	17.78 to 97.40
½"x3/8" M.S.specimens pinned ends	17.3 to 86.6
7/16" dia Al-Mg-alloy specimens fixed ends	20.7 to 130.
7/16" dia Al-Mg-Alloy specimens Pinned ends	20.6 to 118.8
5/8"x5/8" square Al-Mg-alloy specimens pinned ends	18.6 to 82.2

---

* See tables from 13 to 18

.....

4.4. CALCULATING TECHNIQUE AND SPECIMEN CALCULATIONS.

From the simple compressive stress-strain curves drawn in the Appendix, the stress-tangent modulus curves for different materials have been drawn as explained below. On the compressive stress-strain curve various points are taken corresponding to various stresses. On each point, so marked, a tangent is drawn to the compressive stress-strain curve. The slope of the tangent is calculated by dividing the altitude by base of any right angled triangle with the tangent as hypotinuse. The length of altitude and the base are converted into proper* units of stress and strain respectively with the help of the scales on the two axes of the stress-strain diagram prior to dividing altitude by base. The slope of the tangent so calculated gives the tangent-modulus corresponding to the stress represented by the point at which the tangent is drawn. Thus repeating the process for a large number of points on the stress-strain curve we calculated the tangent modulii of the materials for various stress values and the curves of stress-tangent modulus had been drawn for different materials as shown in figure 14, 15, 16 and 17.

It may be added here that slope of the tangents to the compressive stress-strain curve at points taken on curve below the elastic limit, is same throughout as the portion of the curve is straight line, and the slope of this straight portion represents the Young's modulus of that

---

* Stress in-p.s.i. and strain in-(in./in)

particular material.

After calculating the Young's modulus for a particular material and the value of the tangent-modulus at a particular stress level, we can calculate the value of the reduced or double modulus at that stress level by the help of equation No.(6). So knowing the values of tangent and reduced modulii at a particular stress level the slenderness ratios corresponding to the two buckling theories based on the tangent and reduced modulii and represented by the equations (4) and (5) respectively, are calculated. Thus repeating the process for various other stress levels the buckling stress Vs slenderness ratio curves depending upon the two theories are plotted. The specimen calculations are shown below for the material of the round M.S.specimens for "Pinned-end" conditions.

(a) Young's modulus and Tangent modulus calculations.

Young's modulus E = Slope of straight portion of stress-strain curve shown in fig.14

$$= \frac{(14.7 \text{ cm.Altitude}) \times (5000 \text{ psi/cm})}{(0.5 \text{ cm Base}) \times (50 \times 10^{-4} \text{ in/in.per cm})}$$

$$= 29.4 \times 10^6 \text{ p.s.i.}$$

At the stress of 48.5 K.S.i.(Kilo pounds per sq.in.)

Tangent Modulus= E_t = Slope of tangent at the point on stress strain curve for a stress of 48.5 K.S.i.in fig.14.

$$= \frac{(17.7 \text{cm.Altitude}) \times (5000 \text{ psi/cm})}{(1.0 \text{cm Base}) \times (50 \times 10^{-4} \text{ Units of strain/cm})}$$

$$= 17.7 \times 10^6 \text{ p.s.i.}$$

Thus at a stress of 48.5 K.S.i, $E_t = 17.7 \times 10^6$ p.s.i.

(b) "Buckling stress Vs slenderness ratio" curve points on Tangent modulus theory basis.

From eqn. (4) for pinned end conditions

$$\sigma_t = \frac{\pi^2 E_t}{(L/K)^2}$$

$$\text{or } (L/K)^2 = \frac{\pi^2 E_t}{\sigma_t}$$

At the stress of 48.5 K.S.i we have from above

$E_t = 17.7 \times 10^6$ p.s.i.

$$\therefore (L/K)^2 = \frac{\pi^2 \times 17.7 \times 10^6}{(48.5 \times 1000)} = 3600$$

or $L/K = 60$.

Thus for $L/K = 60$ buckling stress on the basis of Engesser's theory $\doteq$ 48.5 K.S.i.

(c) Reduced-modulus calculations:-

From above at the stress 48.5 K.S.i

$E_t = 17.7 \times 10^6$ p.s.i. also for the material.

$E = 29.4 \times 10^6$ p.s.i.

And from equation (6)

$$E_d = \frac{4E_t}{(1+\sqrt{E_t/E})^2}$$

verify if this is true for L.R. circular & rect. cross sec.

$$= \frac{4 \times 17.7 \times 10^6}{(1+\sqrt{17.7 \times 10^6/29.4 \times 10^6})^2}$$

$$= \frac{70.8 \times 10^6}{(1.762)^2} = 22.8 \times 10^6 \text{ p.s.i.}$$

$\therefore$ For stress of 48.5 K.S.i, $E_d = 22.8 \times 10^6$ p.s.i.

(d) "Buckling stress Vs slenderness ratio" curve points on the reduced modulus theory basis.

From above at a stress of 48.5 K.S.i. $E_d = 22.8 \times 10^6$ p.s.i. and from equation No.(5) for "Pinned end" conditions

$$\sigma_d = \frac{\pi^2 E_d}{(L/K)^2}$$

$$\text{or } (L/K)^2 = \frac{\pi^2 E_d}{\sigma_d}$$

$$\text{i.e. } (L/K)^2 = \frac{\pi^2 \times 22.8 \times 10^6}{48.5 \times 1000} = 4560$$

$$\therefore L/K = 67.5$$

Therefore for L/K = 67.5 the buckling stress on the basis of reduced modulus theory = 48.5 K.S.i.

(e) "Buckling stress Vs slenderness ratio" curve points on the Euler's theory basis for Elastic range.

For elastic limit of 48 K.S.i. $E = 29.4 \times 10^6$ p.s.i.

$$\sigma_E = \frac{\pi^2 E}{(L/K)^2} \quad \text{for pinned ends.}$$

$$\text{i.e., } (L/K)^2 = \frac{\pi^2 \times 29.4 \times 10^6}{48 \times 1000} = 5250$$

$$\therefore \quad L/K = 72.5$$

Therefore for L/K = 72.5 the Euler's buckling stress is 48 K.S.i

Thus for various stresses in the elastic as well as plastic range the slenderness ratios are calculated on the basis of tangent and reduced modulii theories of buckling in the plastic range and Euler's theory in the elastic range and tabulated as shown below:

(i) Tangent and reduced modulii curves for material of M.S. round specimens(Carbon Content = 0.178%).

TABLE NO.1.

(Buckling stress Vs slenderness ratio curve for elastic range for the material of M.S. round specimens C=0.178%)

Elastic limit = 48 K.S.i and $E=29.4\times10^6$ p.s.i.

For pinned ends $\sigma_E = \frac{\pi^2 E}{(L/K)^2}$

For fixed ends $\sigma_E = \frac{4\pi^2 E}{(L/K)^2}$

Sr. No.	Buckling stress σ_E K.S.i.	Slenderness ratio (L/K)	
		Pinned ends	Fixed ends
1.	35.6	90;0	180
2.	40.0	85.0	170
3.	45.2	80.0	160
4.	48.0	72.5	155

TABLE NO.2.

(Buckling stress Vs slenderness ratio curve for plastic range for the material of M.S.round specimens,C = 0.178% based on Engesser theory).

For pinned ends $\sigma_t = \frac{\pi^2 E_t}{(L/K)2}$; For fixed ends $\sigma_t = \frac{4\pi^2 E_t}{(L/K)^2}$

Sr. No.	Buckling stress σ_t K.S.i	Tangent Modulus ($E_t \times 10^{-6}$) p.s.i.	SLENDERNESS RATIO L/K	
			Pinned ends	Fixed ends
1.	2.	3.	4.	5.
1.	48.0	29.40	72.50	155.0
2.	48,5	17.70	60.00	120.0

1.	2.	3.	4.	5.
3.	50.0	6.60	36.00	72.0
4.	51.0	3.60	26.30	52.6
5.	52.0	2.00	19.50	39.0
6.	55.0	0.93	12.20	24.4
7.	65.0	0.59	9.45	18.9
8.	75.0	0.396	7.20	14.4
9.	85.0	0.28	5.70	11.4
10.	90.0	0.18	4.44	8.88

TABLE NO.3.

(Buckling stress Vs slenderness ratio curve for plastic range for material of M.S.round specimens C=0.178 based on reduced modulus theory).

For pinned ends $\sigma_d = \frac{\pi^2 E_d}{(L/K)^2}$; For fixed ends $\sigma_d = \frac{4\pi^2 E_d}{(L/K)^2}$

Sr. No.	Buckling stress σ_d K.S.i	Reduced modulus ($E_d \times 10^{-6}$) p.s.i.	Slenderness Ratio L/K	
			Pinned ends	Fixed ends
1.	48.0	29.40	72.50	155.0
2.	48.5	22.80	67.50	135.0
3.	50.0	12.15	48.80	97.6
4.	51.0	7.90	39.0	78.0
5.	52.0	5.03	30.80	61.6
6.	55.0	2.69	21.95	43.9
7.	65.0	1.81	16.55	33.1
8.	75.0	1.27	12.95	25.9
9.	85.0	0.93	10.40	20.8
10.	90.0	0.62	8.25	16.5

(ii) Tangent and Reduced modulii curves for material of M.S.rectangular specimens. Carbon content = 0.485%C.

TABLE No.4.

(Buckling stress Vs slenderness ratio curve for elastic range for the material of M.S.rectangular specmens C=0.485% based on Eulers theory) with pinned end conditions).

Elastic limit = 55 K.S.i. $E=30\times10^6$ p.s.i.

For pinned ends $\sigma_E = \frac{\pi^2 E}{(L/K)^2}$

Sr. No.	Buckling stress σ_E K.S.i	Slenderness ratio L/K
1.	29.7	100.0
2.	36.6	90.0
3.	46.3	80.0
4.	55.0	73.2

TABLE No.5

(Buckling stress Vs slenderness ratio curve for plastic range for M.S.,(C=0.485%), based on the Engesser theory, with pinned end conditions.

For pinned ends $\sigma_t = \frac{\pi^2 E_t}{(L/K)^2}$

Sr. No.	Buckling stress σ_t K.S.i	Tangent modulus $E_t \times 10^{-6}$ p.s.i.	Slenderness Ratio L/K
1.	55.0	30.00	73.2
2.	55.10	27.30	70.0
3.	55.50	20.20	60.0

Table No.5 contd...

1.	2.	3.	4.
4.	56.15	14.20	50.0
5.	58.00	9.40	40.0
6.	60.50	5.51	30.0
7.	63.40	2.56	20.0
8.	68.00	1.54	15.0

E NO.6. Buckling stress Vs slenderness ratio curve for plastic range for M.S.(C=0.485%) based on the reduced modulus theory, with pinned end conditions. $\sigma_d = \pi^2 E_d/(L/K)^2$

Sr. No.	Buckling stress	Reduced modulus $E_d \times 10^{-6}$ p.s.i.	Slenderness ratio L/K
1.	55.25	25.60	67.80
2.	55.50	24.30	65.60
3.	56.00	21.40	61.40
4.	58.00	17.50	54.60
5.	59.00	15.30	50.60
6.	60.00	11.40	43.30
7.	62.00	8.80	37.40
8.	63.00	7.32	33.88
9.	63.50	6.72	32.30
10.	64.0	4.96	27.60
11.	68.0	4.45	30.25
12.	75.0	4.54	24.50
13.	85.0	4.22	22.10
14.	90.0	3.94	20.80

(iii) Tangent and reduced modulii curves for material of Al-Mg-alloy round specimens. Mg.content = 0.755%.

TABLE No.7.

(Buckling stress Vs slenderness ratio curve for elastic range for Al Mg alloy; Mg=0.755%, based on Euler's theory).

Elastic limit = 30 K.S.i; $E=10.7\times10^6$ p.s.i.

For pinned ends $\sigma_E = \frac{\pi^2 E}{(L/K)^2}$

For fixed ends $\sigma_E = \frac{4\pi^2 E}{(L/K)^2}$

Sr. No.	Buckling stress σ_E K.S.i	Slenderness Ratio	
		Pinned ends	Fixed ends
1.	25	65.0	130.0
2.	27	62.5	125.0
3.	30	59.4	118.8

TABLE No.8.

(Buckling stress Vs slenderness ratio curve for plastic range for Al-Mg-alloy, Mg=0.755%, based on Engesser's theory).

For Pinned ends $\sigma_t = \frac{\pi^2 E_t}{(L/K)^2}$; For fixed ends $\sigma_t = \frac{4\pi^2 E_t}{(L/K)^2}$

Sr. No.	Buckling stress σ_t K.S.i	Tangent modulus $E_t \times 10^{-6}$ p.s.i.	Slenderness Ratio L/K	
			Pinned ends	Fixed ends
1.	2.	3.	4.	5.
1.	30.00	10.70	59.40	118.8
2.	30.60	9.40	55.00	110.0
3.	31.60	8.00	50.00	100.0
4.	32.50	6.67	45.00	90.0
5.	33.70	5.43	40.00	80.0

1.	2.	3.	4.	5.
6.	34.70	4.75	35.00	70.0
7.	36.60	3.325	30.00	60.0
8.	38.50	2.45	25.00	50.0
9.	39.60	1.60	20.00	40.0
10.	41.75	0.95	15.00	30.0
11.	42.60	0.65	12.50	25.0
12.	43.3	0.47	10.35	20.7

TABLE No.9.

(Buckling stress Vs slenderness ratio curve for plastic range for Al-Mg-alloy, Mg=0.755% based on reduced modulus theor

For pinned ends $\sigma_d = \frac{\pi^2 E_d}{(L/K)^2}$; For fixed ends $\sigma_d = \frac{4\pi^2 E_d}{(L/K)^2}$

Sr. No.	Buckling stress σ_d =K.S.i.	Reduced modulus $E_d \times 10^{-6}$ p.s.i.	Slenderness Ratio L/K	
			Pinned ends	Fixed ends
1.	2.	3.	4.	5.
1.	30.0	10.70	59.40	118.8
2.	30.4	10.35	57.90	115.8
3.	30.8	9.84	56.10	112.2
4.	31.5	9.20	53.75	107.5
5.	32.2	8.60	51.25	102.5
6.	33.2	7.85	48.20	96.4
7.	34.2	7.05	45.00	90.0
8.	35.7	6.17	41.25	82.5
9.	37.4	5.10	36.70	73.4
10.	39.2	3.90	31.25	62.5
11.	41.4	2.35	23.60	47.2
12.	43.0	1.35	17.60	35.2
13.	44.0	1.00	15.00	30.0
14.	46.0	0.62	11.60	23.2

(iv) Tangent and reduced modulii curves for material of Al-Mg-alloy square specimens-Mg content =0.808%.

TABLE No.10.

Buckling stress Vs slenderness ratio curve for elastic range for Al-Mg alloy, (Mg=0.808%), based on Euler's theory with pinned ends.

Elastic limit = 34 K.S.i; $E=10.6\times10^6$ p.s.i.

For pinned ends $\sigma_E = \frac{\pi^2 E}{(L/K)^2}$

Sr. No.	Buckling stress σ_E K.S.i.	Slenderness ratio L/K.
1.	15.4	85.0
2.	21.4	70.0
3.	29.0	60.0
4.	34.0	55.4

TABLE NO.11.

(Buckling stress Vs slenderness ratio curve for plastic range for Al-Mg-alloy, Mg=0.808% based on reduced modulus theory with pinned end).

For pinned ends $\sigma_d = \frac{\pi^2 E_d}{(L/K)^2}$

Sr. No.	Buckling stress σ_d K.S.i	Reduced Modulus $E_d \times 10^{-6}$ p.s.i.	Slenderness Ratio L/K
1.	34.0	10.60	55.40
2.	34.5	9.00	50.60
3.	37.0	4.95	36.00
4.	39.0	3.72	30.65
5.	43.0	1.85	20.60
6.	45.0	0.723	12.65
7.	50.0	0.37	8.50

TABLE No.12.

(Buckling stress Vs slenderness ratio curve for plastic range for Al-Mg-alloy, Mg=0.808%, based on tangent modulus theory with pinned ends).

For pinned ends $\sigma_t = \frac{\pi^2 E_t}{(L/K)^2}$

Sr. No.	Buckling stress σ_t K.S.i	Tangent Modulus $E_t \times 10^{-6}$ p.s.i.	Slenderness ratio L/K
1.	34.0	10.60	55.40
2.	34.5	7.70	46.90
3.	35.0	4.72	36.40
4.	37.0	2.85	27.60
5.	39.0	1.88	21.80
6.	41.0	1.13	16.50
7.	43.0	0.74	13.00
8.	44.0	0.48	10.40
9.	45.0	0.24	7.25
10.	46.0	0.176	6.14
11.	48.0	0.06	3.54
12.	50.0	0.038	2.74

4.5 EXPERIMENTAL RESULTS

(a) Table No.13 (Experimental Results for fixed-ends round M.S. specimens 7/16" dia, Carbon = 0.178%)

The machine was operated on 20-ton scale for first four readings and on 5-ton scale for rest of the readings.

Sr. No.	Mean Diameter Inches	End to end length Inches	Lengh for calculations Inches	Slenderness ratio = L/K = 4L/d	Load-zero -error Tons	Buckling load(Observed) Tons	Buckling load (corrected) From Fig. 14&13 lbs.	Buckling Stress K.S.I.	Remarks
1.	2.	3.	4.	5.	6.	7.	8.	9.	10.
1.	0.437	2.235	1.875	17.11	0.36	7.670	16480	110.0	
2.	0.4368	2.234	1.874	18.08	0.36	6.900	14700	97.8	
3.	0.4371	3.23	2.87	26.24	0.36	4.500	9290	61.8	
4.	0.4370	3.236	2.876	26.3	0.36	4.280	8850	59.0	
5.	0.4370	3.236	2.876	26.3	0.332	4.540	11700	78.0	
6.	0.4373	3.249	2.889	26.42	0.332	4.530	11700	78.0	
7.	0.437	4.612	4.252	38.9	0.332	3.920	10000	66.5	
8.	0.4386	4.608	4.248	38.8	0.332	3.900	9950	65.8	
9.	0.4380	4.624	4.264	38.9	0.33	3.710	9450	62.3	
10.	0.4381	5.498	5.138	46.85	0.33	3.500	9075	60.0	

Contd...

1.	2.	3.	4.	5.	6.	7.	8.	9.	10.
11.	0.4381	5.496	5.136	46.80	0.33	3.435	8650	57.0	
12.	0.4376	6.624	6.264	57.2	0.33	3.232	8500	56.0	
13.	0.4376	6.619	6.259	57.1	0.33	3.234	8500	56.0	
14.	0.4371	7.621	7.261	66.4	0.33	3.190	8000	53.3	
15.	0.4368	7.629	7.269	66.6	0.33	3.160	7900	52.5	
16.	0.4377	8.755	8.395	76.8	0.33	3.450	8700	57.8	
17.	0.4371	8.752	8.392	76.8	0.33	3.435	8650	57.4	
18.	0.4372	9.884	9.524	87.2	0.34	2.900	7000	46.5	
19.	0.4373	9.880	9.520	87.2	0.34	3.070	7625	50.8	
20.	0.4373	11.000	10.640	97.4	0.34	3.084	7700	51.2	
21.	0.4365	11.005	10.645	97.5	0.34	2.870	7075	47.0	
22.	0.4373	12.009	11.649	106.6	0.34	3.010	7475	49.5	
23.	0.4374	12.008	11.648	106.6	0.34	3.050	7575	52.2	
24.	0.4363	12.998	12.640	116.0	0.34	2.910	7200	47.9	
25.	0.4375	14.00	13.640	125.0	0.34	2.878	7100	47.1	
26.	0.4373	13.999	13.640	125.0	0.34	2.710	6625	44.0	
27.	0.435	15.127	14.767	135.8	0.34	2.710	6625	44.5	

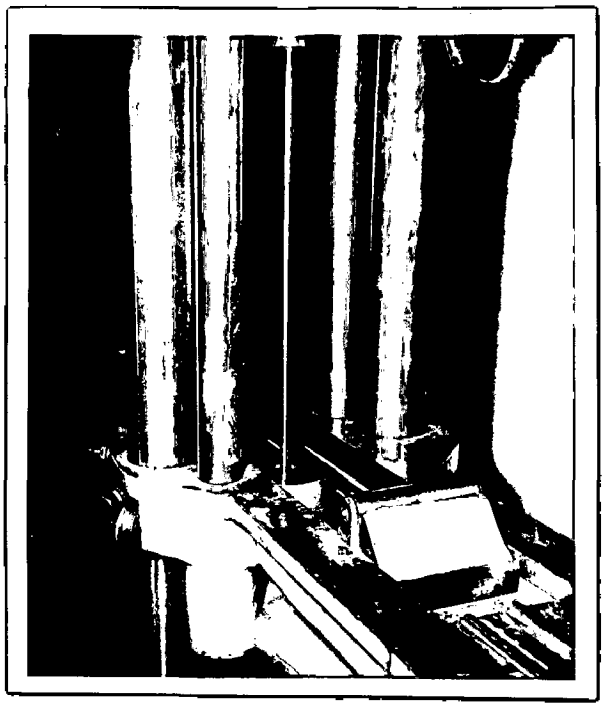

Round specimen with fixed ends before buckling.

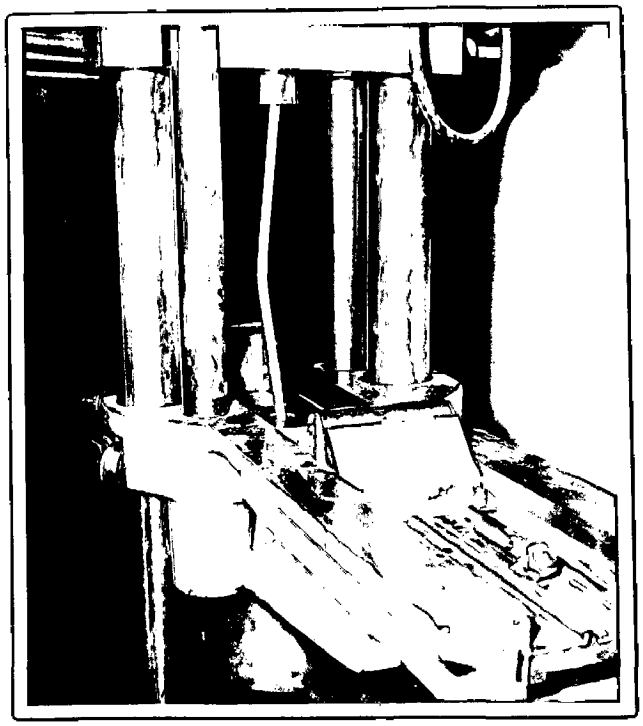

Round specimen with fixed ends after buckling.

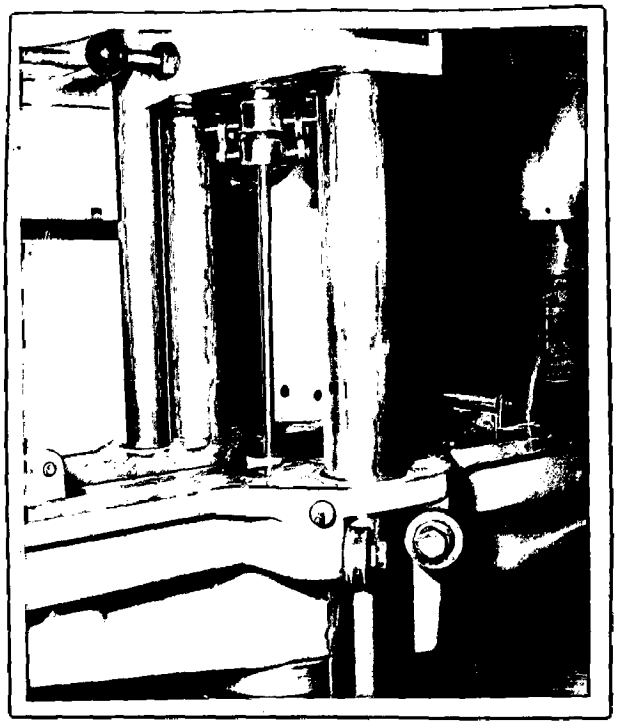

Round specimen with pinned ends before buckling.

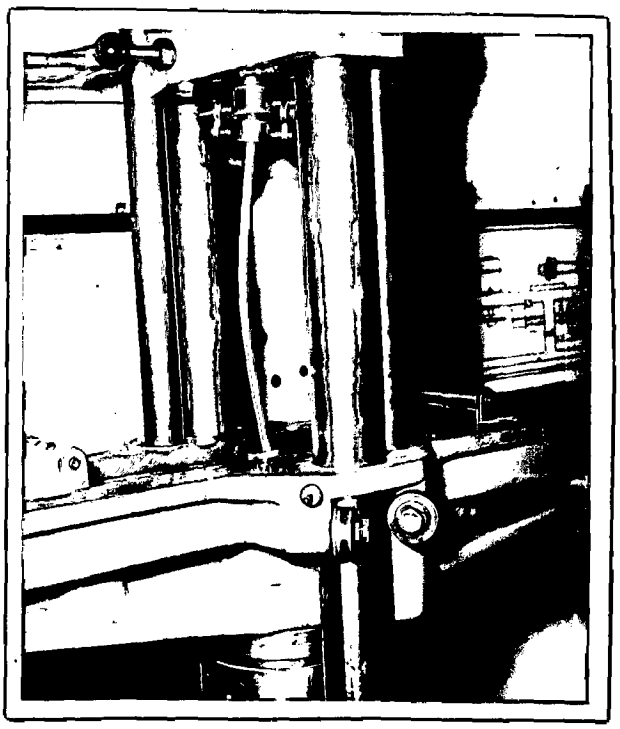

Round specimen with pinned ends after buckling.

(b) Table No.14 (Experimental results for Pinned-ends round M.S. Specimens 7/16" Dia, Carbon = 0.178%)

The machine was operated on 5 ton-scale.

Sr. No.	Mean Dia Inches	Length of test piece, L Inches	Distance between ball centres L_1 Inches	Slenderness Ratio $\frac{L}{K}=\frac{4L}{d}$	Slenderness Ratio $\frac{L_1}{K}=\frac{4L_1}{d}$	Zero Error Tons	Observed Buckling load Tons	Actual Buckling load from curve of Fig.-13 lbs.	Buckling stress K.S.I.	REMARKS
1.	2.	3.	4.	5.	6.	7.	8.	9.	10.	11.
1.	0.4367	1.940	4.190	17.78	38.40	0.335	3.530	7120	47.5	
2.	0.4368	1.953	4.203	17.85	38.50	0.335	3.870	7950	53.0	
3.	0.4361	1.945	4.195	17.83	38.50	0.335	3.685	7500	50.2	
4.	0.4379	1.940	4.190	17.73	38.30	0.330	3.750	7030	46.8	
5.	0.4376	2.874	5.124	26.30	47.00	0.340	3.160	6320	42.0	
6.	0.4374	2.885	5.135	26.40	47.00	0.340	3.360	6760	44.8	
7.	0.4370	2.880	5.130	26.30	47.00	0.340	3.300	6630	44.2	
8.	0.4373	2.879	5.129	26.40	46.95	0.330	3.290	6630	44.2	
9.	0.4377	4.180	6.430	38.20	58.80	0.330	3.720	7580	50.2	
10.	0.4378	4.179	6.429	38.20	58.75	0.330	3.540	7180	47.6	

1.	2.	3.	4.	5.	6.	7.	8.	9.	10.	11.
11.	0.4378	5.024	7.274	45.90	66.50	0.330	3.565	7185	47.6	
12.	0.4377	5.005	7.255	45.70	66.40	0.335	3.425	6920	46.0	
13.	0.4366	6.150	8.400	56.40	76.90	0.335	3.452	6970	46.5	
14.	0.4377	6.155	8.405	56.40	76.80	0.330	3.460	7000	46.6	
15.	0.4365	7.130	9.380	65.30	85.80	0.330	2.885	5720	37.5	
16.	0.4374	7.116	9.366	65.10	85.60	0.335	2.857	5650	37.6	
17.	0.4373	8.205	10.455	75.00	95.60	0.330	2.740	5400	35.8	
18.	0.4359	8.187	10.437	75.00	95.60	0.330	3.090	5950	39.8	
19.	0.4365	9.355	11.605	85.80	106.40	0.330	2.587	5050	33.7	
20.	0.4370	9.336	11.586	85.40	106.00	0.330	3.120	6240	41.5	
21.	0.4366	9.352	11.602	85.80	106.40	0.330	2.577	5030	33.7	
22.	0.4373	10.655	12.905	97.40	118.50	0.330	2.895	5750	38.3	
23.	0.4376	10.634	12.884	97.30	117.80	0.330	2.622	5130	34.3	
24.	0.4376	10.640	12.890	97.30	117.90	0.330	2.567	5000	33.3	

(c) Table No.15 (Experimental Results for Pinned end rectangular M.S. specimen

Carbon = 0.485%, $\frac{1}{2}$" x $\frac{3}{8}$")

The machine was operated on 20-Ton scale

Sr. No.	Mean Breadth In.	Mean Depth In.	Length of Test piece L In.	Distance between ball centres L_1 In.	Slenderness Ratio $\frac{L_1}{K}$	Slenderness Ratio $\frac{L_1/\sqrt{12}}{d}$	Slenderness Ratio $\frac{L_1}{K}$	Slenderness Ratio $\frac{L_1/\sqrt{12}}{d}$	Zero Error Tons	Observed buckling load Tons	Actual buckling load from Fig.14 Tons	Buckling stress K.S.I.	Remarks
1.	2.	3.	4.	5.	6.		7.		8.	9.	10.	11.	12.
1.	0.5000	0.3750	1.871	4.121	17.30		38.1		0.36	5.84	5.52	66.00	
2.	0.4995	0.3755	1.875	4.125	17.35		38.2		0.36	5.56	5.25	62.60	
3.	0.5006	0.3750	1.875	4.125	17.35		38.2		0.36	5.69	5.38	64.20	
4.	0.4980	0.3749	2.733	4.983	25.20		45.8		0.36	5.64	5.33	64.00	
5.	0.5000	0.3751	2.884	5.134	26.60		47.3		0.36	5.82	5.47	64.70	
6.	0.5000	0.3715	2.876	5.126	26.80		47.8		0.36	5.94	5.63	66.00	
7.	0.4994	0.3765	4.003	6.253	36.80		57.5		0.36	4.60	4.25	50.70	Test piece No.7 instrumented with strain gauges. The deflection of voltmeter
8.	0.4994	0.3752	4.000	6.250	37.00		57.8		0.36	5.48	5.17	61.80	
9.	0.5000	0.3996	4.824	7.074	41.90		61.5		0.36	4.81	4.50	49.80	

1.	2.	3.	4.	5.	6.	7.	8.	9.	10.	11.	12.
10.	0.5001	0.3993	4.860	7.110	42.20	61.7	0.36	4.58	4.27	47.8	needle was 5½
11.	0.4960	0.3710	6.097	8.347	56.90	78.0	0.36	4.47	4.11	50.10	divisions(On the 100 division scale)
12.	0.4986	0.3741	6.068	8.318	56.60	77.7	0.36	4.56	4.25	50.80	upto buckling load when it incr-
13.	0.5001	0.3740	7.259	9.509	67.30	88.0	0.36	4.84	4.53	54.00	eased abruptly
14.	0.5000	0.3740	7.262	9.512	67.30	88.0	0.36	4.50	4.19	50.10	to the extreme end.
15.	0.4930	0.3740	8.085	10.335	74.80	95.8	0.36	4.70	4.39	52.50	instrumented Test piece No.15/
16.	0.4996	0.3750	8.085	10.335	74.60	95.7	0.36	5.10	4.79	57.40	with strain gauges
17.	0.4960	0.4020	9.173	11.423	79.00	98.5	0.36	3.98	3.66	41.00	The deflection of
18.	0.4960	0.3996	9.160	11.400	79.30	98.5	0.36	3.22	2.88	32.40	voltmeter needle
19.	0.5003	0.4010	9.148	11.398	78.95	98.0	0.36	3.98	3.66	41.00	was 7 division(on
20.	0.5010	0.3960	9.165	11.415	79.00	98.5	0.36	3.29	2.98	33.70	the 100 div.scale)
21.	0.4976	0.4030	9.902	12.152	85.10	104.3	0.36	3.78	3.44	38.50	upto buckling load
22.	0.4986	0.3870	9.905	12.155	85.50	104.3	0.36	3.77	3.43	38.45	when it increased
23.	0.4995	0.4000	9.915	12.165	85.90	105.0	0.36	3.84	3.51	39.40	abruptly to extrem
24.	0.4975	0.3963	9.908	12.158	86.60	106.5	0.36	3.58	3.25	37.00	end.

(d) Table No.16 (Experimental results for the Pinned ends round 7/16" Al - Mg alloy specimens. Mg. Content = 0.755%)

The machine was operated on 5-ton scale.

Sr. No.	Mean Dia. In.	Length In.	Slenderness Ratio $\frac{L}{K} = \frac{4L}{d}$	Zero Error Tons	Observed buckling load Tons	Actual buckling load from Fig. 13. lbs.	Buckling stress K.S.I.	Remarks
1.	2.	3.	4.	5.	6.	7.	8.	9.
1.	0.4389	2.256	20.6	0.37	2.84	6975	46.07	
2.	0.4380	2.250	20.6	0.37	3.02	7400	48.9	
3.	0.4389	3.261	29.7	0.37	2.84	6975	46.0	
4.	0.4389	3.260	29.7	0.37	2.56	6150	40.6	
5.	0.4397	4.650	42.4	0.37	2.66	6400	42.4	
6.	0.4405	4.655	42.4	0.37	2.76	6700	44.2	
7.	0.4399	5.528	50.3	0.37	2.35	5000	37.0	
8.	0.4399	5.520	50.3	0.37	2.73	6600	43.5	
9.	0.4399	6.636	60.5	0.37	2.58	6200	41.2	
10.	0.4375	6.630	60.6	0.37	2.60	6250	41.5	
11.	0.4370	7.625	69.7	0.37	2.16	5025	33.5	

1.	2.	3.	4.	5.	6.	7.	8.	9.
12.	0.4374	7.660	70.0	0.33	2.290	5225	34.60	
13.	0.4376	8.777	80.3	0.33	2.038	4800	31.90	
14.	0.4385	9.884	90.2	0.33	1.558	3500	23.30	
15.	0.4383	9.873	90.1	0.33	1.740	3975	26,40	
16.	0.4380	10.977	100.0	0.33	1.518	3375	22.40	
17.	0.4385	10.976	100.0	0.33	1.430	3100	20.50	
18.	0.4374	12.000	109.5	0.33	1.215	2500	16.60	
19.	0.4381	12.000	109.2	0.33	1.200	2475	16,35	
20.	0.4386	13.016	118.8	0.33	0.880	1575	10.40	
21.	0.4382	13.000	118.8	0.33	1.140	2400	15.90	

(e) Table No.17 (Experimental results for the fixed-ends round 7/16" AL-Mg alloy specimens Mg content = 0.755%

The machine was operated on 5-ton scale

Sr. No.	Mean Dia In.	End to end Length of Test piece In.	Effective length for calculations In.	Slenderness ratio $\frac{L}{K} = \frac{4L}{d}$	Zero Error Tons	Observed buckling load Tons.	Actual buckling load from Fig.13 lbs.	Buckling stress K.S.I.	Re - ma- r- ks
1.	2.	3.	4.	5.	6.	7.	8.	9.	10
1.	0.4395	2.636	2.276	20.70	0.332	2.895	7150	42.2	
2.	0.4390	2.636	2.76	20.71	0.332	2.872	7120	47.1	
3.	0.4392	2.640	2.280	20.76	0.332	2.877	7125	47.1	
4.	0.4379	2.640	2.280	20.77	0.332			No result was	
5.	0.4392	3.632	3.272	29.80	0.332	2.533	6220	41.0 obtained as the	
6.	0.4390	3.629	3.269	29.75	0.332	2.526	6150	40.65 electric supply	
7.	0.4386	3.628	3.268	29.20	0.332	2.528	6150	40.8 went off and	
8.	0.4386	3.640	3.280	29;90	0.332	2.558	6225	41.3 the machine	
9.	0.4393	5.009	4.649	42.20	0.332	2.395	5725	37.8 stopped.	
10.	0.4391	4.999	4.639	42.10	0.332	2.400	5825	39.4	

Contd.....

1.	2.	3.	4.	5.	6.	7.	8.	9.	10.
11.	0.4380	5.904	5.544	50.6	0.332	2.380	6400	42.6^{0}	
12.	0.4381	5.895	5.535	50.5	0.332	2.660	5850	43.2^{0}	
13.	0.4380	7.013	6.653	60.7	0.332	2.472	6000	39.7^{0}	
14.	0.4371	7.040	6.680	61.0	0.332	2.392	5700	37.8^{0}	
15.	0.4376	8.044	7.684	70.3	0.330	2.200	5250	35.0^{0}	
16.	0.4392	8.016	7.656	69.7	0.330	2.160	5125	33.8^{0}	
17.	0.4372	9.140	8.780	80.3	0.330	2.205	5200	34.6^{0}	
18.	0.4371	9.154	8.794	80.5	0.330	2.055	4800	31.94	
19.	0.4379	10.259	9.899	90.4	0.332	1.932	4500	29.00	
20.	0.4395	10.234	9.874	89.8	0.332	2.370	4520	29.60	
21.	0.4382	11.353	10.993	100.3	0.332	2.022	4450	28.3^{0}	
22.	0.4370	11.352	10.992	100.5	0.332	2.920	4740	29.9^{0}	
23.	0.4382	12.360	12.000	109.7	0.332	1.845	4250	28.25	
24.	0.4377	12.390	12.030	109.8	0.332	1.760	4050	26.90	

Contd....

1.	2.	3.	4.	5.	6.	7.	8.	9. 10.
25.	0.4372	13.390	13.030	119.5	0.330	1.630	3650	24.25
26.	0.4380	13.380	13.020	119.2	0.330	1.700	3850	25.60
27.	0.4377	14.580	14.220	130.0	0.330	1.420	3100	20.00
28.	0.4372	14.570	14.210	130.0	0.330	1.430	3150	21.00

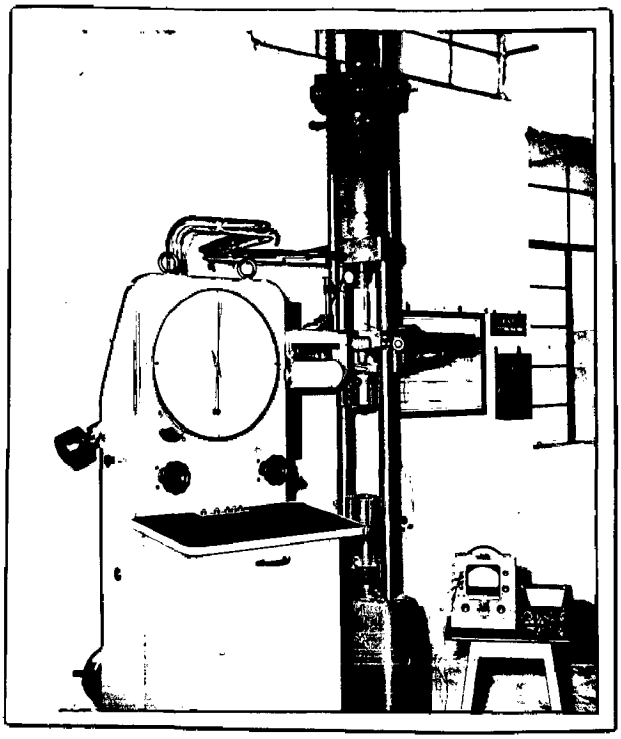

Instrumented rectangular specimen with pinned ends before buckling.

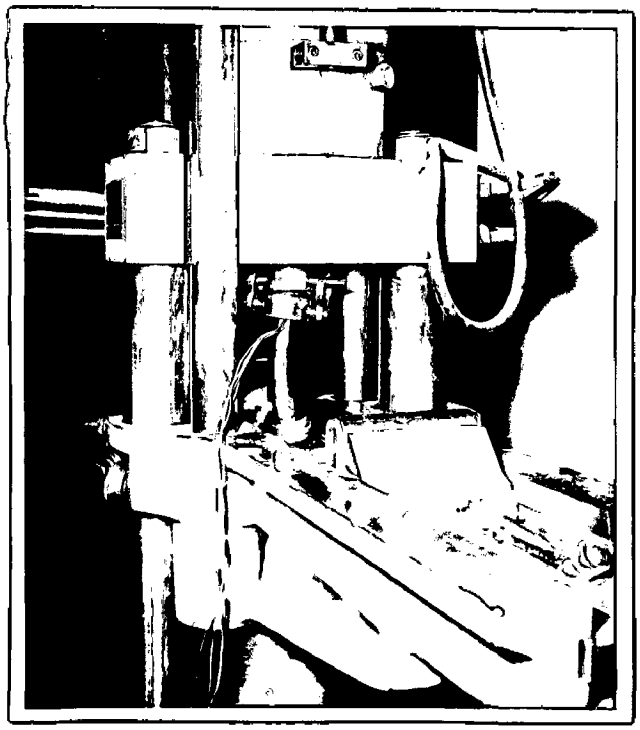

Instrumented rectangular specimen with pinned ends after buckling.

(f) Table No.18 (Experimental results for the Pinned-ends square $\frac{5"}{8}$ x $\frac{5"}{8}$ Al.-Mg. alloy Mg = 0.808%)

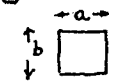

The machine was operated on 20 ton scale

$\frac{L}{K} = \frac{\sqrt{12}L}{a}$ if a < b and $\frac{L}{K} = \frac{\sqrt{12}L}{b}$ if b < a

Sr. No.	Mean Edge 'a' In.	Mean Edge 'b' In.	Length of Test piece L In.	Slenderness Ratio $\frac{L}{K}$	Zero Error Tons	Observed buckling load Tons	Actual buckling load from Fig. 14 Tons	Buckling stress K.S.I.	Remarks
1.	2.	3.	4.	5.	6.	7.	8.	9.	10.
1.	0.6245	0.6243	3.530	18.60	0.36	7.47	7.16	41.2	
2.	0.6240	0.6246	3.326	18.45	0.36	7.44	7.13	41.1	
3.	0.6230	0.6247	4.529	25.20	0.36	7.74	7.43	42.4	
4.	0.6227	0.5610	4.528	25.20	0.36	6.86	6.55	42.0	Test piece No.4
5.	0.6238	0.6240	5.605	31.10	0.36	7.39	7.08	40.7	instrumented with
6.	0.6242	0.6225	5.864	32.50	0.36	7.47	7.16	41.2	strain gauges. The
7.	0.6234	0.6242	5.873	32.60	0.36	6.59	6.28	36.2	deflection of volt-
8.	0.6254	0.6252	6.988	38.80	0.36	5.98	5.67	32.5	meter needle was
									4 Div.(on the 100 Div.
									scale) upto buckling

1.	2.	3.	4.	5.	6.	7.	8.	9.	10.
									load when it increased abruptly to the extreme.
9.	0.6247	0.5627	6.985	38.80	0.36	6.98	6.67	42.6	Test piece No.9 instru-
10.	0.6227	0.6251	9.284	51.80	0.36	4.20	3.84	22.1	mented with strain gauge:
11.	0.6240	0.6247	9.279	51.50	0.36	5.75	5.44	31.4	The deflection of volt-
12.	0.6248	0.6243	12.560	69.60	0.36	7.73	3.37	19.5	meter-needle was 7 Div.
13.	0.6250	0.6243	12.560	69.60	0.36	5.34	4.98	28.8	(on the 100 Div.scale)
14.	0.6197	0.6173	17.063	95.00	0.36	2.12	1.76	10.3	upto buckling load
15.	0.6240	0.6232	17.062	94.80	0.36	2.65	2.29	13.2	when it increased abrup-
16.	0.6220	0.6217	18.310	102.00	0.36	2.62	2.26	13.0	tly to the extreme.
17.	0.6240	0.6243	20.310	113.00	0.36	2.21	1.85	10.65	
18.	0.6240	0.6247	5.617	31.20	0.36	7.72	7.36	42.6	
19.	0.6252	0.6230	12.250	68.00	0.37	5.73	5.40	31.1	
20.	0.6220	0.6250	13.120	73.00	0.37	3.12	2.75	15.8	
21.	0.6190	0.6250	14.680	82.20	0.37	3.35	3.00	17.3	

FIG 4. BUCKLING CURVES OF M.S. $\frac{3}{4}$" DIA. ROLLED RODS.
COMPOSITION :- 0·178 % CARBON

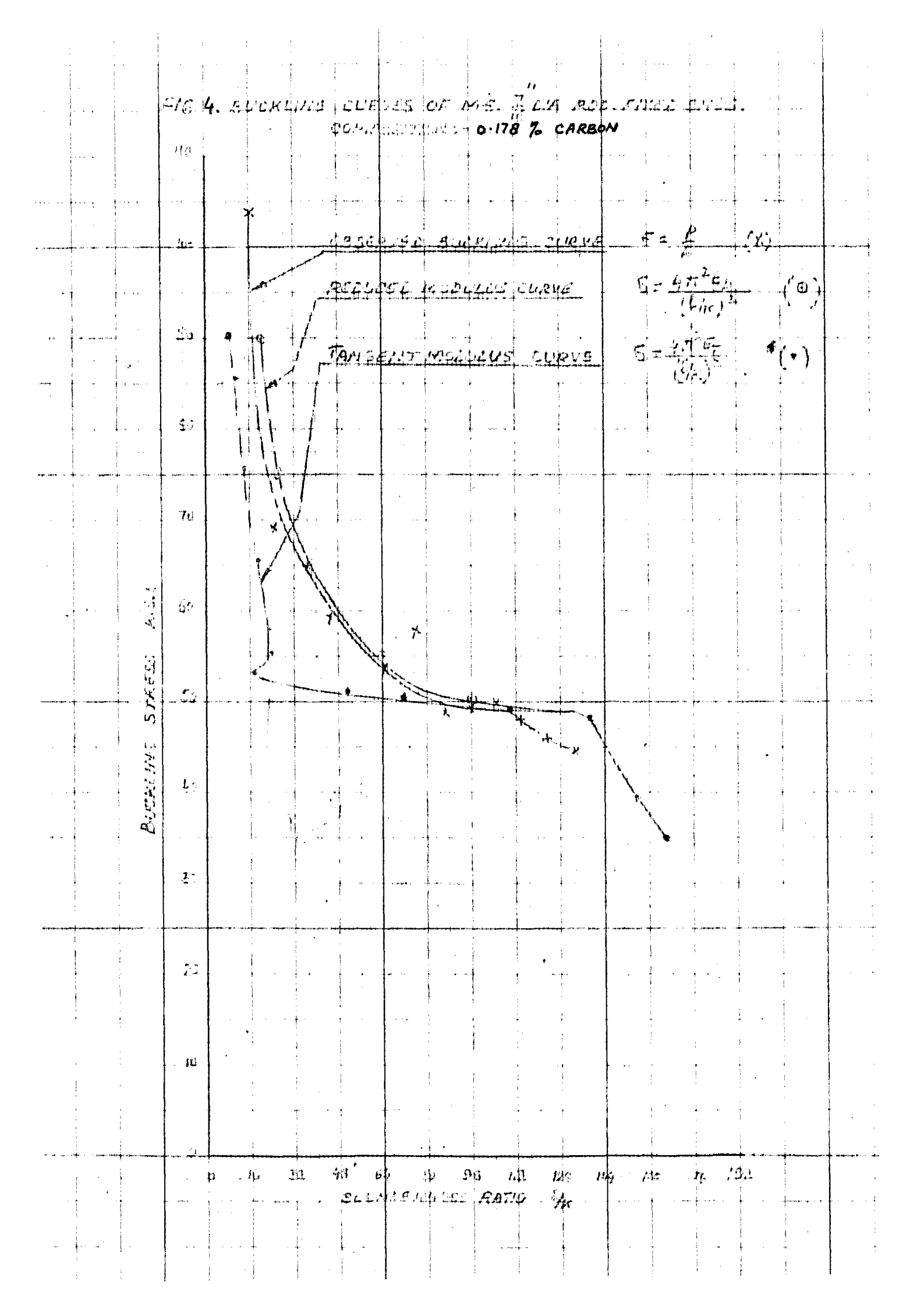

FIG 5 BUCKLING CURVES OF $\frac{7}{16}$" DIA. M.S. RODS. PINNED ENDS.
COMPOSITION :- 0.178 % CARBON.

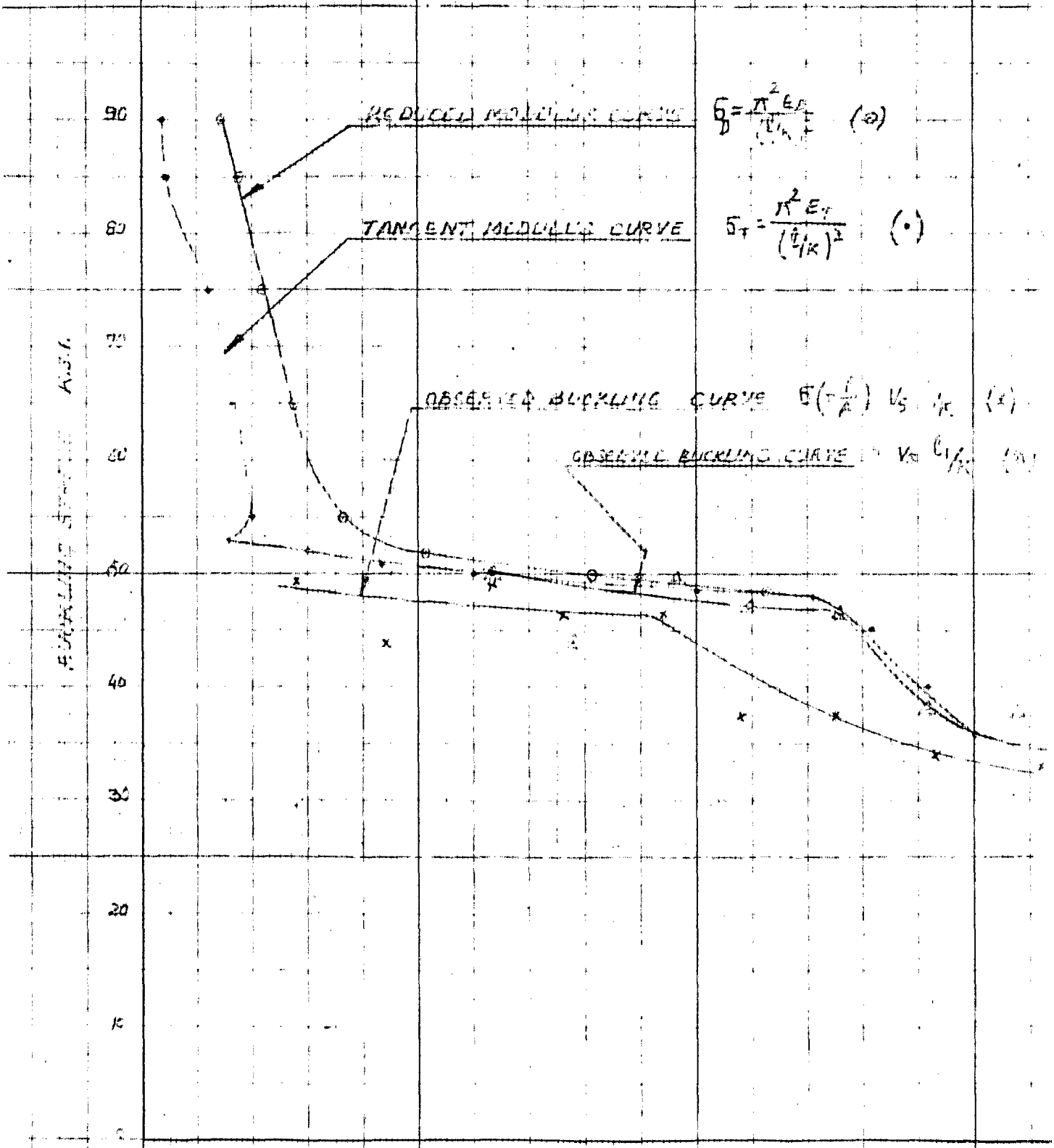

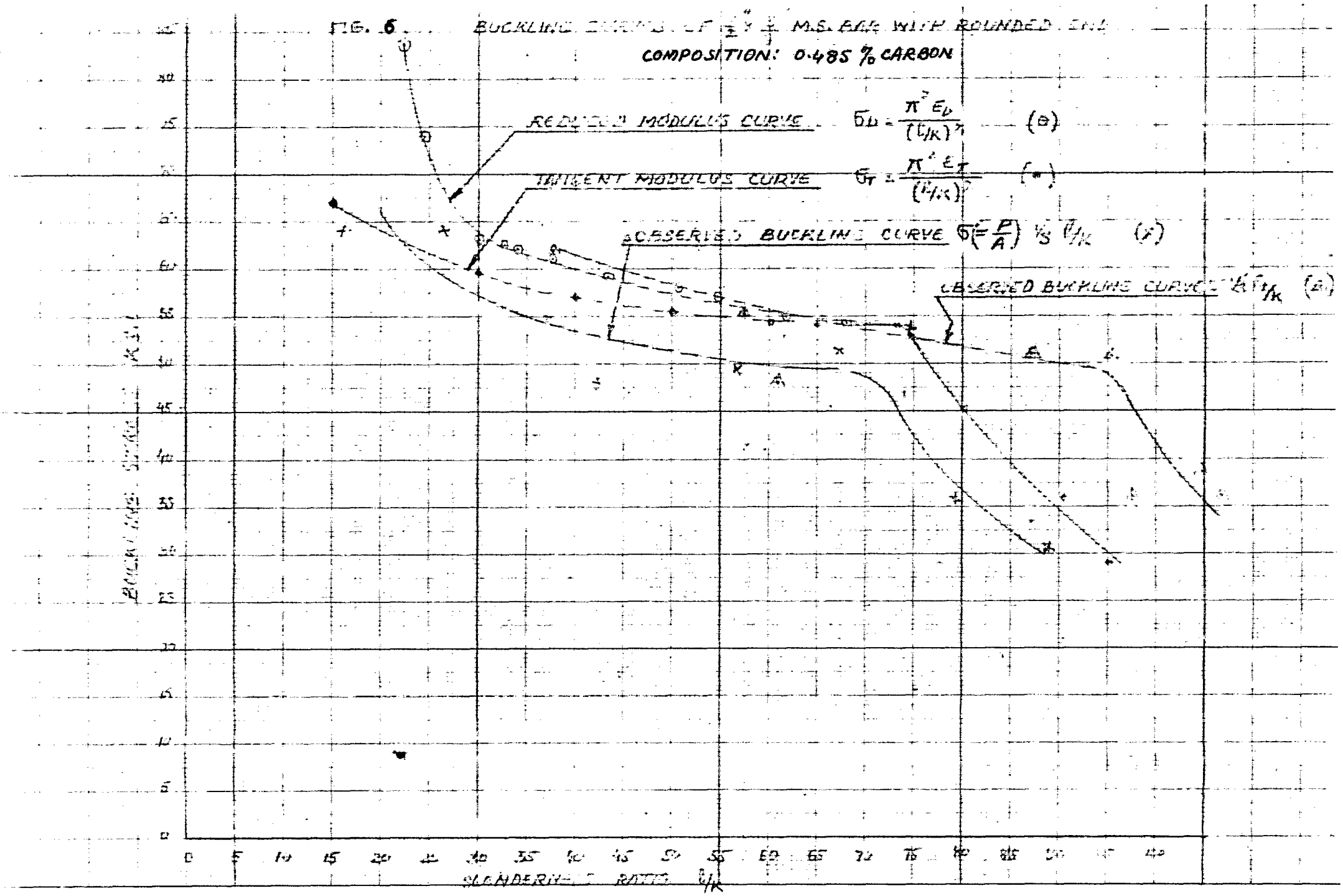
FIG. 6 BUCKLING CURVES OF ½" ϕ M.S. BAR WITH ROUNDED ENDS
COMPOSITION: 0.485 % CARBON
REDUCED MODULUS CURVE $\sigma_D = \frac{\pi^2 E_D}{(l/k)^2}$ (a)
TANGENT MODULUS CURVE $\sigma_T = \frac{\pi^2 E_T}{(l/k)^2}$ (e)
OBSERVED BUCKLING CURVE $\sigma (= \frac{P}{A})$ Vs l/k (f)
OBSERVED BUCKLING CURVE Vs l/k (g)
BUCKLING STRESS KG/MM²
SLENDERNESS RATIO l/k

FIG- 7) BUCKLING CURVES OF Al-Mg ALLOY. $\frac{7}{16}$" DIA FIXED ENDS

COMPOSITION:- 0·755 % Mg

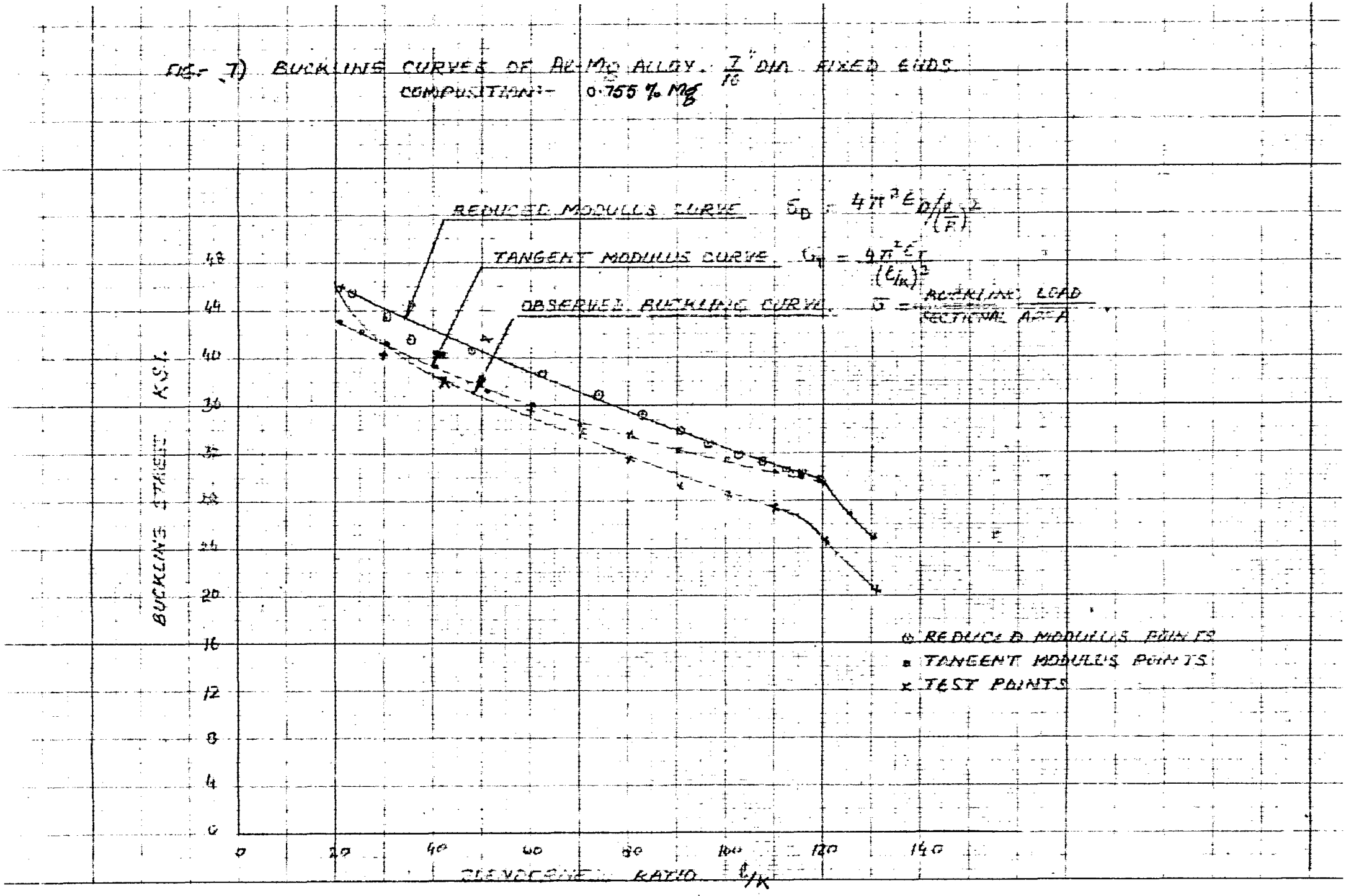

FIG-8. BUCKLING CURVES OF Al-Mg ALLOY. $\frac{1}{16}$ D.A. PINNED ENDS.

COMPOSITION: 0.755 % Mg

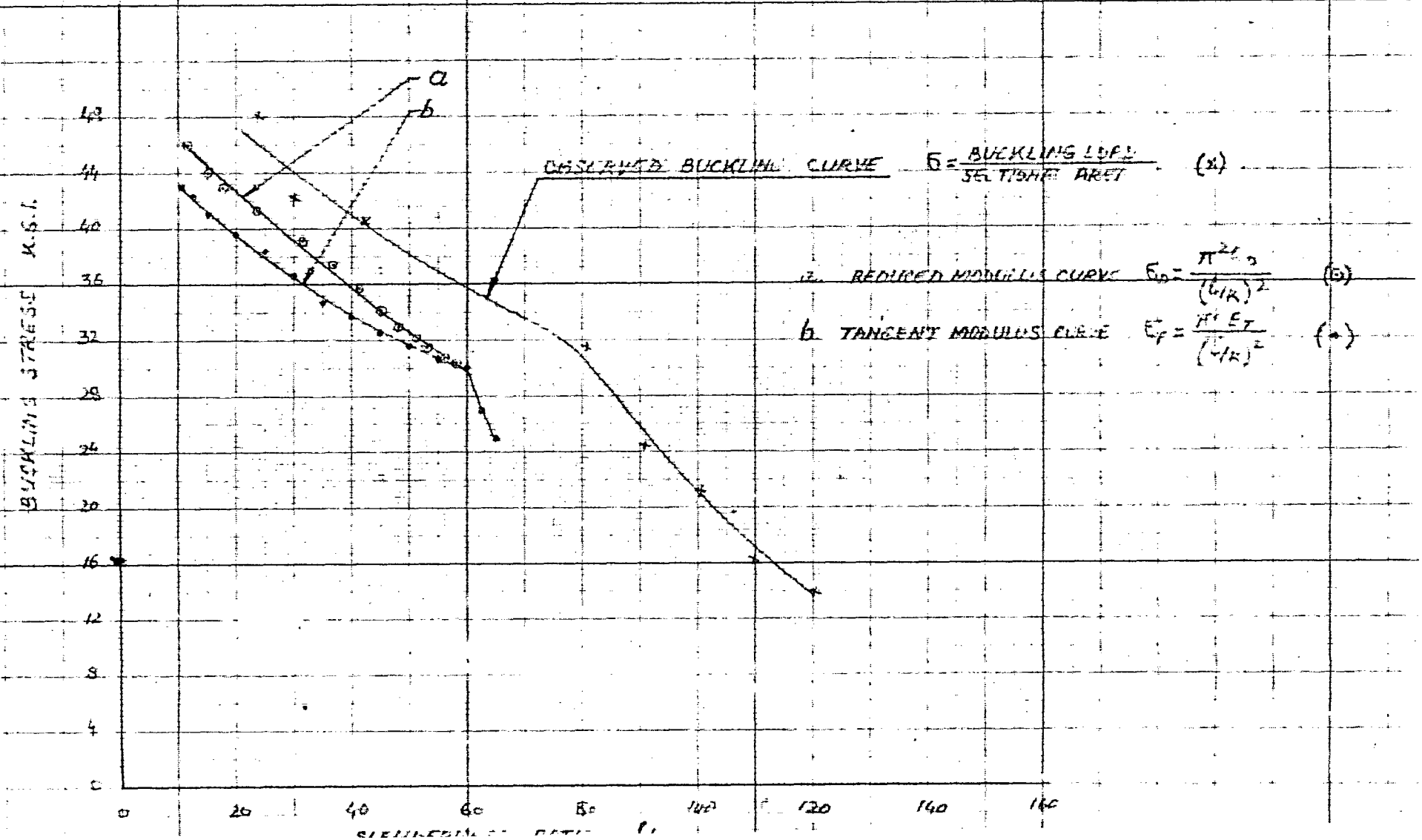

OBSERVED BUCKLING CURVE $\sigma = \frac{\text{BUCKLING LOAD}}{\text{SECTIONAL AREA}}$ (a)

a. REDUCED MODULUS CURVE $\sigma_b = \frac{\pi^2 E_0}{(l/k)^2}$ (b)

b. TANGENT MODULUS CURVE $E_T = \frac{\pi^2 E_T}{(l/k)^2}$ (c)

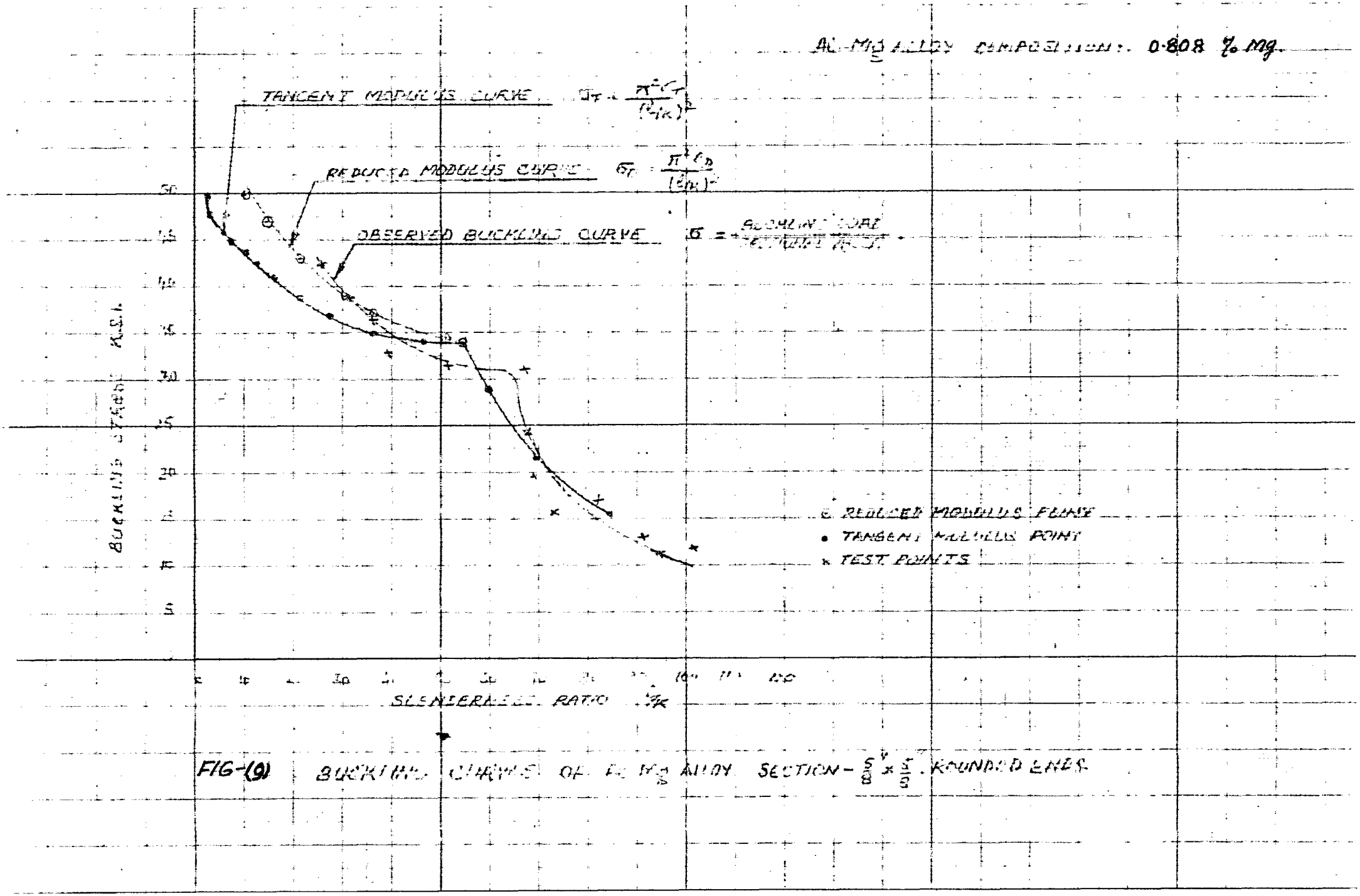

FIG-(9) BUCKLING CURVES OF Al Mg ALLOY SECTION - $\frac{5}{8}$" x $\frac{1}{16}$" ROUNDED EDGES

FIG. 10 BUCKLING STRESSES COMPARED FOR DIFFERENT END CONDITIONS OF ROUND ½" DIA MILD STEEL COLUMNS.

COMPOSITION : 0·178 % CARBON

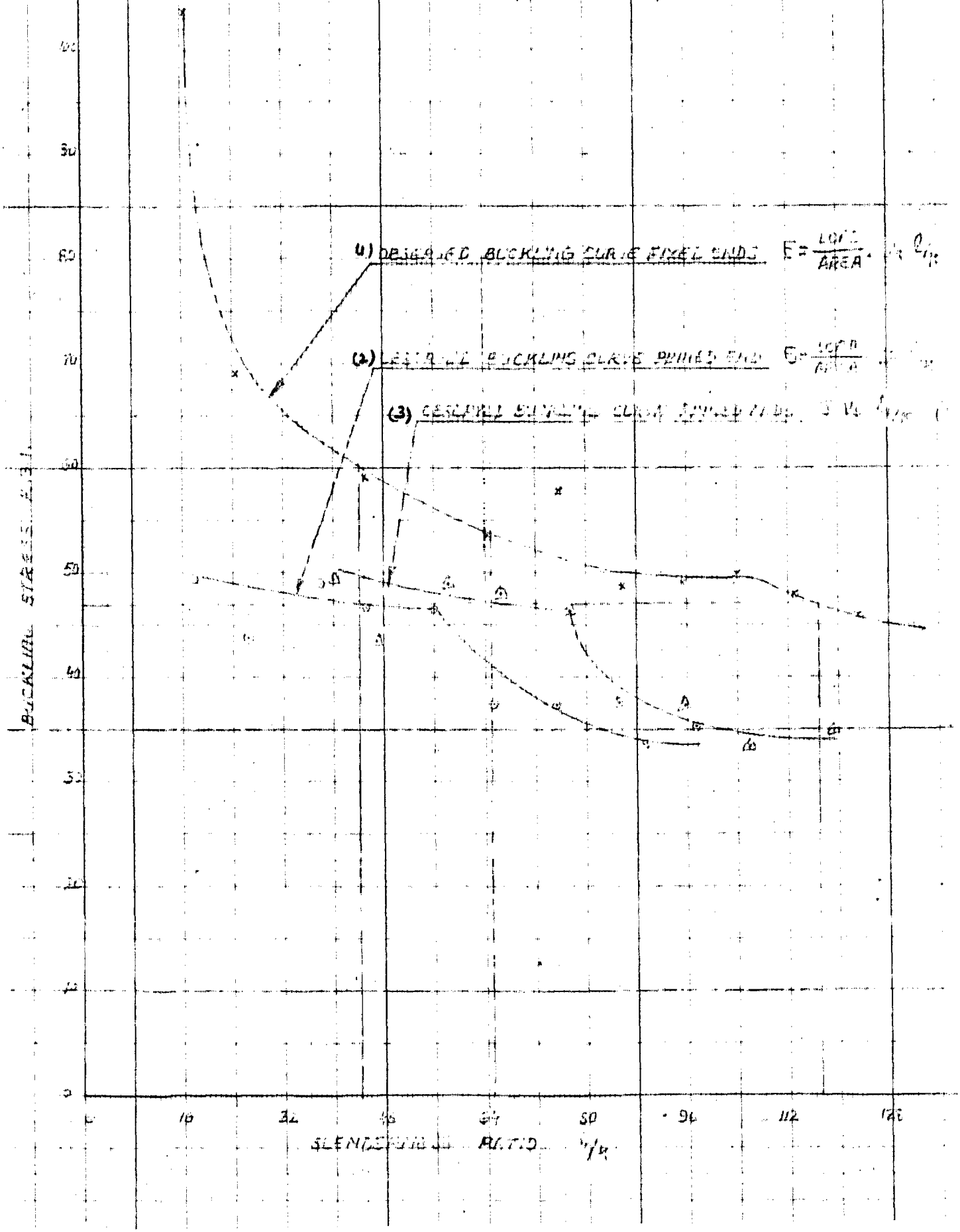

FIG-11. BUCKLING STRESS COMPARED FOR DIFFERENT END CONDITIONS OF Al Mg ALLOY $\frac{1}{16}$" DIA.

COMPOSITION = 0·755 % Mg.

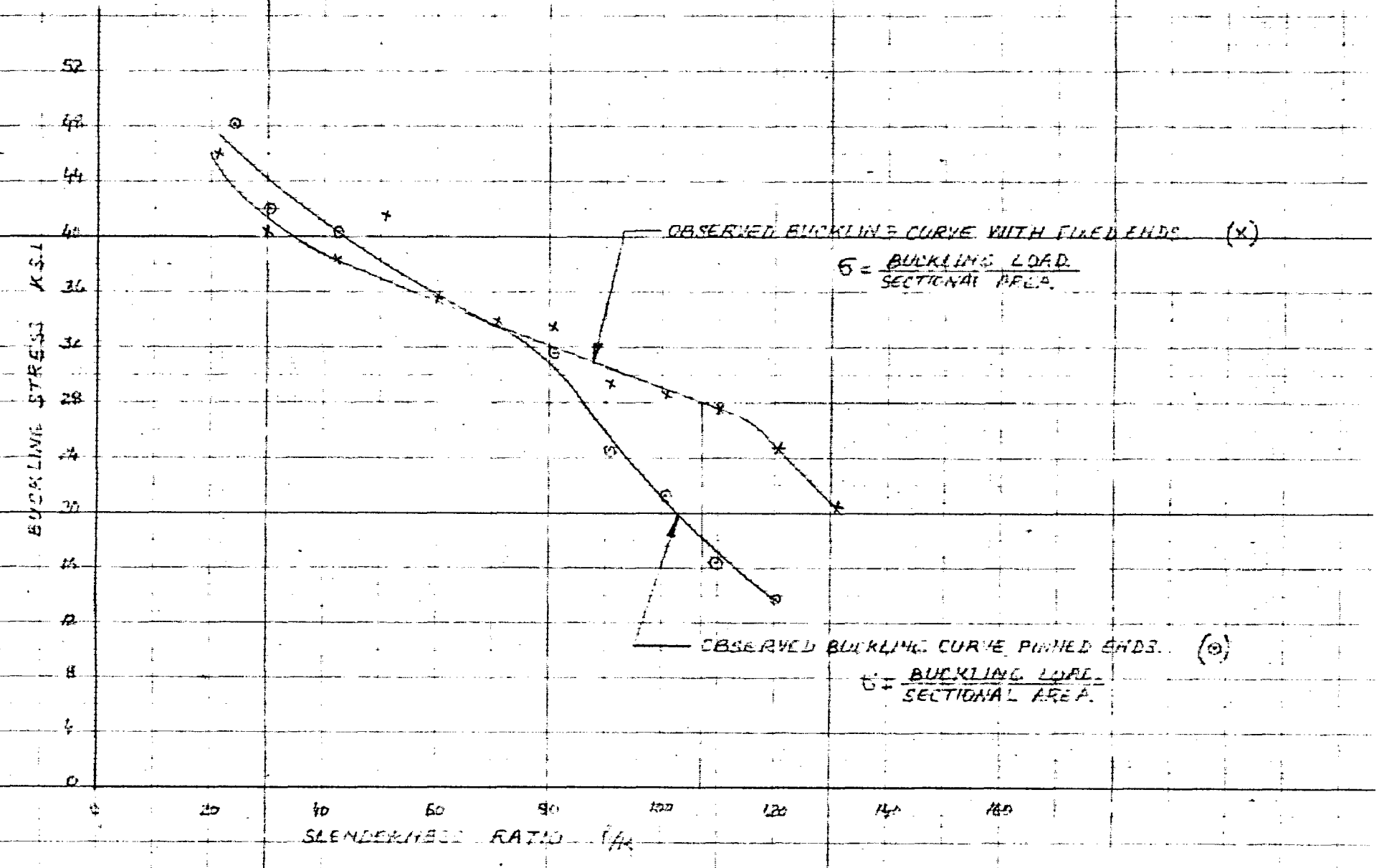

4.6 Discussion of Results

4.6(a) Buckling curves discussions

(1) Buckling curve for Round M.S. specimens with Fixed ends (Fig.

The buckling curve for the round 7/16 in. dia M.S. specimens (Carbon = 0.178%) with fixed ends condition is drawn in Fig. No.4 on the basis of the observations tabulated in table No.13 Super-imposed on this observed buckling curve are two theoretical curves viz. tangent-modulus and reduced modulus curves plotted on the basis of the values given in tables (1), (2) and (3).

From these curves we observe that for the buckling stresses below the elastic limit, the observed buckling stress has a lower value as compared to the theoretical Euler's stress. The reason for this small deviation may be that the specimens have a little eccentricity due to manufaturing tolerances in the fixture as well as in the proper turning of test pieces due to which a bending moment is induced on the specimens thereby causing them to criple down at a relatively low stress.

For the plastic range we observe from the actual curve that the buckling stress remains practically constant as the slenderness ratio reduces from 108 to 87, and side by side it is very slightly below the tangent-modulus buckling curve. As the slenderness ratio reduces below 87 to 16 the actual buckling stress goes on increasing and the curve lies near to but slightly below the reduced modulus buckling curve and above the tangent modulus curve.

This behavior of the material can be explained as below.

For the inelastic range the increase in buckling stress beyond the Euler's value, will depend upon the variation of the tangent modulus with increasing stress. In the highly curved region of the compressive stress-strain diagram of the material (see Fig. 15), the tangent modulus drops very rapidly with the increase of stress; consequently very little increase in buckling stress would be obtained and as such for the 'perfect' concentric columns the buckling curve in the plastic range just beyond the knee of the compressive stress-strain curve, should coincide with the tangent-modulus curve. But for the little eccentricity which creeps in due to manufacturing tolerances the actual curve is slightly below the theoretical tangent modulus curve.

In the so called plastic range, beyond the knee of the compressive stress-strain diagram the tangent modulus has a relatively low value and does not change rapidly with the increasing stress (see Fig. 15). Thus from the equation No.(6), keeping in view that youngs modulus E is constant, we have for low values of tangent modulus E_t, relatively large increase in the value of reduced modulus E_D, with the increasing stress. Therefore the buckling stress is approaching the one predicted by the double modulus theory in the so called plastic range beyond the knee of the stress-strain diagram. But in actual testing of columns, there is some eccentricity due to manufacturing tolerances due to which a bending moment is induced on the test pieces so the actual observed curve is slightly below

the theoretical double-modulus curve. Secondly the observed curve with the so-called fixed ends condition may not represent the true picture due to the slip that might have occured at the ends thereby tending to bring down the actual curve little below the theoretical one.

It has already been pointed out in the review of literature that for M.S. and other materials for which the compressive stress-strain curve has a flat portion, beyond the elastic limit, for a sufficient length, the buckling stress Vs slenderness ratio curve will be horizontal in the plastic range. But here we see that the actual buckling curve (see Fig. 4) remains practically horizontal only for a small portion of the curve beyond the elastic range, and then rises up with the decrease in slenderness ratio. This can be explained on the basis of the actual compressive stress-strain curve of the material (M.S. - 0.178% Carbon) as shown in Fig. 14. This curve beyond the yield point remains horizontal only for a comparatively smaller length so that the corresponding plastic strains induced in the material, before it gets strain hardened, might not be sufficient to make the column buckle as anticipated earlier.

(ii) Buckling curve for round AL-Mg.alloy specimens (Mg = 0.755%) with fixed ends. (Fig. 7)

The buckling curve for the round 7/16 in. dia. Al-Mg alloy specimens (Mg = 0.755%) with fixed ends condition is drawn in Fig. 7 on the basis of observations tabulated in table No.17. Superimposed on this observed buckling curve are two theoretical curves, viz. tangent modulus and reduced modulus curves plotted from the values given in

tables (7) and (8).

From these curves we observe that for the buckling stresses below the elastic limit, the observed buckling stress- has a lower value as compared to the theoretical Euler's stress. The reason for this deviation of the observed values from the theoretical ones may be that the specimens have a little eccentricity due to manufacturing tolerances in the fixture as well as in the proper turning of the test specimens due to which a bending moment is induced on the specimens thereby causing than to criple down at a relatively low stress. Secondly the slip at so called fixed ends, might have occured thereby tending to bring down the actual curve below the theoretical one.

For the plastic range we observe from the actual buckling curve that the buckling stress increases from 26.8 K.S.I. to 38.4 K.S.I. with the decrease of slenderness ratio L/K from 114 to 40 in more or less a straight line fashion beyond which the curve starts rising along a pretty highly curved path to a stress value of 46 K.S.I. at a slenderness ratio of 20. Mostly the observed buckling curve in the plastic range is below even the tangent modulus curve; only at the slenderness ratio of 30 and corresponding buckling stress 41.2 K.S.I. it crosses the tangent modulus curve and there meets the reduced modulus curve at a buckling stress of 46 K.S.I. corresponding to L/K = 20. This behavior can be explained as under.

As pointed above, for the plastic range the increase in buckling stress beyond the Euler's value depends on the variation of the tanget modulus with increasing stress. In

the highly curved region of the stress-strain diagram, the tangent modulus drops rapidly with the increaseof stress (see Fig. 17); consequently the increase in the buckling stress with the decrease in slenderness ratio will not be a sharp one and as such for the perfect columns the buckling curve should coincide with the tangent modulus curve. But for the little eccentricity which creeps in due to manufacturing tolerances the actual curve is slightly below the theoretical tangent modulus curve. This is what we are observing as mentioned above.

In the so called plastic range, beyond the knee of the compressive stress-strain curve, the tangent modulus has a relatively low value and does not change rapidly with the increasing stress (see Fig. 17). Thus from the equation No.6, keeping in view that youngs modulus E is constant, we have for low values of tangent modulus E_t, relatively large increase in the value of the reduced modulus E_D, with the increasing stress. Therefore the buckling stress is approaching the one predicted by the double modulus in the so called plastic range beyond the knee of the compressive stress strain diagram. This is what we are observing as mentioned above. The slight deficiency in the approach of the observed buckling curve to the theoretical double modulus curve may be due to some eccentricity which might have crept in due to manufacturing tolerances. Secondly due to the slip that might have occured in the so called fixed ends, the observed curve might have been brought down slightly below the theoretical curve.

(iii) Buckling curve for round 7/16" M.S. specimens (0.178% Carbon) with pinned ends

The buckling curve σ Vs L/K for the round 7/16 in. dia. M.S. specimens (0.178% Carbon) with pinned-ends condition is drawn in Fig. 5. Superimposed on this curve (σ Vs L/K) are two theoretical curves plotted on the basis of the values given in tables (1), (2), and (3). The observed buckling stress Vs L/K curve shows two distinct regions, evidently one elastic and the other plastic. The elastic region ends at a stress value of 46.5 K.S.I. corresponding to slenderness ratio, L/K of 55.8. The plastic region curve shows slight increase in the stress from 46.5 to 48 K.S.I. with corresponding decrease in slenderness ratio from 55.8 to 13.8. In addition the plastic region curve is almost parallel to the tangent modulus curve for this range of slenderness ratio but it is little below the tangent modulus curve. The slight downward displacement of the observed curve from the tangent modulus curve may be explained as below.

As discussed above a perfect column will follow the tangent modulus curve for the stresses for which the corresponding points lie just beyond the knee of the compressive stress-strain curve. But here it may be due to the eccentricity which is introduced by the manufacturing tolerances, due to which a bending moment is set up on the test specimens and in turn the buckling load is reduced. But even then the deviation from the tangent modulus curve is pretty high, and more particularly the deviation for the elastic region is much pronounced. This marked deviation

is explained on the grounds that the physical length of the column is not the representative for the numerator in the expression (L/K) for slenderness ratio because the actual bending of the column takes place about the centres of the balls of the pinned-end fixture shown in Fig. 2. Moreover the length of the swivelling blocks of the pinned-ends fixture is not a negligible quantity and as such it is even more than the lengths of a few specimens of low slenderness ratio. Further if we take distance between centres of balls of the fixture shown in Fig. 2, L_1, and devide by the radius of gyration to get the value of the slenderness ratio, even then it will not be correct, because in that case the swivelling blocks having very large cross-sectional area will not bend as the test specimen does, rather they will form straight links between the bent specimen and centres of balls. Thus we can infer that the true length to be substituted for the numerator in the expression, (L/K) for slenderness ratio will be some where in between L and L_1 where L is the physical length of the test specimen (excluding snugs) and L_1 the distance between the balls' centres when the test specimen of length L is held inthe pinned end fixture as shown in Fig. 2. Mathematically the problem has been analysed under the heading "Mathematical Analysis", where it has been shown that the true "Buckling stress Vs slenderness ratio" curve will lie below the one in-which L_1 represents the numerator of the expression for slenderness ratio and above the one in which 'L' is taken into account. More so the curve in which L_1 is considered is a better approximation. Therefore to see this effect the buckling stress Vs L_1/K curve has been

added in Fig. 5. From the Fig. 5 also we observe this σ Vs L_1/K curve approaches very well to the theoretical curve for the elastic as well as for the plastic range also. It is very slightly away from the tangent modulus curve and this very small deviation may be attributed to the eccentricity which might have crept in due to manufacturing tolerances.

(iv) Buckling curve for rectangular ½" x 3/8" M.S. specimens (0.485% Carbon) with pinned ends.

The buckling curve σ Vs L/K for the rectangular ½" x 3/8" M.S. specimens (0.485% Carbon) with pinned-ends condition is drawn in Fig. 6. Superimposed on this curve (σ Vs L/K) are two theoretical curves plotted on the basis of the values given in the tables 4, 5 and 6. The observed buckling stress Vs L/K curve shows two distinct regions, evidently one elastic and the other plastic. The elastic region ends at a stress value 49.5 K.S.I. corresponding to slenderness ratio of 67. The plastic region curve shows an increase in stress from 49.5 K.S.I. to 66 K.S.I. with the corresponding decrease in slender-ness ratio from 67 to 20. In the plastic region just beyond the elastic region the curve is parallel but sufficiently below the tangent modulus curve, but later on for higher values of stress or for lower values of slenderness ratio the curve is almost parallel to the double modulus curve but again it is sufficiently below the reduced modulus curve also. As discussed above from the theoretical considerations we expect a perfect column to follow the tangent modulus curve for the stresses for which the corresponding points lie just beyond the knee, of the compressive stress-strain-curve

and in the later stages i.e. for points sufficiently for off from the knee the perfect column will follow the double-modulus curve. But here in the actual σ Vs L/K curve the deviations might be firstly due to the eccentricity which is introduced by the manufacturing tolerances, due to which a bending moment is set up on the test-Specimens and in turn the buckling load is reduced. Secondly the marked deviation may be explained as done above for M.S. round specimens with pinned-ends on the grounds that the physical length of the column is not the representative for the numerator in the expression L/K, for slenderness ratio because the actual bending of the column takes place about the centres of the balls of the pinned-end fixture shown in Fig. 2. Moreover the length of the swivelling blocks of the pinned-ends fixture is not a negligible quantity and as such it even more than the lengths of a few specimens of low slenderness ratio. Further if we take distance between centres of balls of the pinned-end fixture shown in Fig.(2), L_1, and devide by the radius of gyration to get the value of slenderness ratio, it will not be free from error because in that case the swivelling blocks having very large cross-sectional area will not bend as the test specimen does, rather they will form straight links between the bent specimen and centres of balls. Thus we can infer that the true length to be substituted for the numerator in the expression, L/K, for slenderness ratio will be some where in between L and L_1 there 'L' is the length of test specimen and 'L_1' the distance between the labbs' centres when the test specimen of length 'L' is held in the pinned-ends fixture as shown in Fig. 2. Even mathematically this [illegible]

under the heading "Mathematical analysis". Therefore to see this effect, here also, the buckling stress σ Vs L_1/K curve has been added in figure No.6. From the figure No.6 we observe that the observed curve is shifted to the right if drawn on the basis of L_1/K as slenderness ratio. As such for the same slenderness ratio the values of the buckling stress as predicted by this σ Vs L_1/K curve are greater than even the double modulus values in plastic range and the Euler's values in the elastic range, which in itself seems to be not in confirmity of any of the theoretical curves. This can be explained on the basis of the fact that, L_1, as pointed above is not the true figure to be used in the expression for slenderness ratio but a value little less than L_1 and little greater than L is to be taken.

From these we noted that the observed stress-slenderness ratio curve moves more nearer to the curves obtained on the basis of the available theories.

V. Buckling curve for round 7/16 in. dia Al-Mg-alloy(0.755% Mg) with pinned ends:

The buckling curve σ Vs L/K for the round 7/16 in. dia Al-Mg alloy(0.755% Mg) with pinned-ends condition is drawn in figure 8. Superimposed on this curve (σ Vs L/K) are two theoretical curves plotted on the basis of the values given in table 4,5 & 6.

From the figure 8 we see that the observed buckling curve is parallel to tangent modulus curve as far as its plastic range is concerned and separately parallel to the Euler's curve for its elastic range. Secondly the observed

curve is far above the two theoretical curves, this behaviour seems to be quite abnormal. The reason for this may be that the so called pinned-ends fixture might have not been behaving like the true pinned-ends fixture because the experiment on the Al-Mg-alloy round specimens was performed last of all and by that time slight depressions had been introduced in the conical cavities of the fixture blocks and these defaced conical cavities would have increased the friction thereby giving fixing moments at the ends and thus giving higher buckling loads than the actual ones. Thus we can conclude that the observed curve will actually be much below than its present position in figure 8. As such originally it is already parallel to the tangent-modulus curve we may conclude that it might have been very near to the theoretical tangent modulus curve if the friction-less end conditions were prevailing.

VI. Buckling curve for square (5/8"x5/8") Al-Mg-alloy (Mg=0.808%) specimens with pinned ends.

The buckling curve σ Vs L/K for the 5/8" square section Al-Mg-alloy (0.808% Mg) with pinned ends condition is drawn in figure 9. Superimposed on this curve (σ Vs L/K) are two theoretical curves plotted on the basis of the values given in tables 10,11 and 12. The observed buckling stress Vs L/K curve shows two district regions; evidently one elastic and the other plastic. The observed curve lies very close to the theoretical curves but it is slightly above them at few points. This little deviation may be due to slight friction at the balls and conical cavities, which tend to shift the observed curve upwards.

Therefore within the experimental limitations there is close approximation between the observed and theoretical curves. For the smaller values of slenderness ratio the observed curve tends to follow the reduced modulus curve and for values of slenderness ratio such that the buckling stress is in the plastic region and close to the knee the tangent modulus curve is approached.

(4.6 b) Mathematical analysis of the buckling of the pinned-end specimens.

A specimen held in the swivelling blocks is shown in the limiting position in the figure No.12.

Let L_1 = The distance between the centres of balls.

a = Length of the swivelling blocks

h_o = The central deflection

y = The deflection at any distance x from the lower ball centre A where the origin is assumed to lie.

In case if it is assumed that the swivelling blocks also bend to the same shape as if it was a continuous column of uniform section from A to B, the shape of the slightly bent column in the limiting case can be taken as

$$Y = h_o \sin \frac{\pi X}{L_1} \qquad \ldots\ldots\ldots\ldots\ldots\ldots (7)$$

The curvature at any point of the column in the deflected position is given by

$$\frac{1}{\rho} = \frac{d^2y/dx^2}{\left[1+\left(\frac{dy}{dx}\right)^2\right]^{3/2}} \qquad \ldots\ldots\ldots\ldots\ldots\ldots (8)$$

Now from equation (7) we have

$$dy/dx = h_o \frac{\pi}{L_1} \cos \frac{\pi x}{L_1} \qquad \ldots\ldots (9)$$

and $d^2y/dx^2 = -\frac{h_o\pi^2}{L_1^2} \sin \frac{x}{L_1}$ .....(10)

$\therefore$ From (9) and (10)

$\therefore$ Slope at A = $(dy/dx)_{x=0} = h_o \frac{\pi}{L_1}$ ....(11)

and $(d^2y/dx^2)_{x=0} = 0$ .....(12)

$\therefore$ From (11)&(12) curvature at A=Curvature at B.

$= (1/\rho)_{x=0} = 0$ .....(13)

Thus the curvature at the ball centres of the ideal curve will be zero.

Now to find the curvature of the ideal, uniform pinned end column at a distance 'a' from A, we have, from (9) and (10).

$$(dy/dx)_{x=a} = h_o \frac{\pi}{L_1} \cos \frac{a\pi}{L_1} \quad \ldots\ldots\ldots\ldots (14)$$

$$\text{and } (d^2y/dx^2)_{x=a} = -h_o \frac{\pi^2}{L_1^2} \sin \frac{a\pi}{L_1} \quad \ldots\ldots\ldots\ldots (15)$$

$\therefore$ The curvature at a distance 'a' from the ends of the perfect column is given with the help of equations (8), (14) and (15)

$$(1/\rho)_{x=a} = \frac{-h_o \frac{\pi^2}{L_1^2} \sin \frac{a\pi}{L_1}}{\left[1 + h_o^2 \frac{\pi^2}{L_1^2} \cos^2 \frac{a\pi}{L_1}\right]^{3/2}} \quad \ldots\ldots(16)$$

The expression no.(16) as such is quite complicated to solve and hence will be examined with special conditions.

(a) Firstly let $a \ll L_1$ i.e., in our practical column when the length of the swivelling blocks separately is very small as compared to the distance between the centres

of balls or in other words for very slender columns.

Then we have $\frac{a\pi}{L_1}$ to be a small quantity

i.e., Sin $\frac{a\pi}{L_1}$ tends to $\rightarrow$ $\frac{a\pi}{L_1}$

and Cos $\frac{a\pi}{L_1}$ tends to $\rightarrow$ 1

$\therefore$ Equation (16) reduces to

$$(1/\rho)_{x=a} \simeq \frac{-h_o \frac{\pi^2}{L_1^2} \times \frac{a\pi}{L_1}}{\left(1+ h_o^2 \frac{\pi^2}{L_1^2}\right)^{3/2}}$$

$$= -a \frac{h_o}{L_1^3}\pi^3 \left[1- \frac{3}{2} \frac{h_o^2}{L_1^2} + \ldots\ldots\right]$$

Now neglecting the terms with the higher powers of (h_o/L_1) being very small

$$(1/\rho)_{x=a} \simeq -a \frac{h_o \pi^3}{L_1^3} \ldots\ldots\ldots\ldots(17)$$

From equation (17) we see that the magnitude of curvature of centre line of a perfect ℄ pinned end column of length L_1 at a small distance 'a' from the end is $\frac{a\, h_o \pi^3}{L_1^3}$, which is a very small quantity because h_o is very small and L_1 is very large.

Thus we see that in the case of practical columns of very high slenderness ratio, the fact that "the swivelling blocks do not bend" does not affect the results for the buckling curve calculated on the basis of the distance between centres of balls being taken as the actual length of the column.

(b) Secondly considering the case when the distance L_1 is not very large as compared to 'a' ⅓ the length of the swivelling

blocks i.e., in practical cases of very stocky columns.

Taking the actual values of 'a' for the shortest column of all the various series of test performed with the hinged ends condition, we have

$$a \simeq L_1/4 \qquad \text{.....(18)}$$

Then from equations (16) and (18)

$$(1/\rho)_{x=a} = \frac{-h_o \frac{\pi^2}{L_1^2} \sin \frac{\pi}{4}}{\left[1 + h_o^2 \frac{\pi^2}{L_1^2} \cos^2 \frac{\pi}{4}\right]^{3/2}}$$

$$\text{or } (1/\rho)_{x=a} = \frac{-h_o \frac{\pi^2}{L_1^2} \times 1/\sqrt{2}}{\left[1 + \frac{\pi^2 h_o^2}{2L_1^2}\right]^{3/2}} \qquad \text{.....(19)}$$

Equation (19) will be looked upon for two extreme cases

(i) when $\frac{\pi^2 h_o^2}{2L_1^2} \gg 1$

i.e., when $h_o^2 > L_1^2/5$ approx.

i.e., when $h_o \quad L_1/\sqrt{5}$ .....(20)

Now the least value of L_1 in our practical column is 4 in.

$\therefore$ the relation (20) reduces to

i.e., when $h_o > 4/\sqrt{5}$

or when $h_o > 1.8$ in.

which is in contradiction from the very definition of neutral equilibrium condition in a slightly deflected position, for the buckling load acting on the column. Thus the condition $\pi^2 h_o^2/2L_1^2 \gg 1$ does not hold good.

(ii) When $\pi^2 h_o^2/2L_1^2 \ll 1$

Then equation (19) reduces to

$$(1/\rho)_{x=a} = -h_o \frac{\pi^2}{L_1^2} 1/\sqrt{2} \left(1 - \frac{3}{2} \frac{\pi^2 h_o^2}{2L_1^2} + \ldots\ldots\right)$$

$$\simeq -h_o \frac{\pi^2}{L_1^2} \times 1/\sqrt{2}$$ Neglecting the terms with higher powers of (h_o^2/L_1)

$$\text{i.e., } (1/\rho)_{x=a} \simeq -6.96 \frac{h_o^2}{L_1^2} \quad \ldots\ldots\ldots(21)$$

For the least value of $L_1 = 4$ in. Equation 21 reduces to

$$(1/\rho)_{x=a} = -\frac{6.96}{16} h_o^2$$

$$= -0.434\ h_o^2 \quad \ldots\ldots\ldots\ldots\ldots(22)$$

Since h_o has maximum value limited to some thousandths of an inch, the value of the curvature given by equation (22) even, is very small. Also from equation (13) we see that the curvature at the ball centres is zero. Thus from equations 13, 17,19 and 22 we see that the curvature does not change appreciably from the ball centres to the point x=a i.e., the change of curvature from the ball centres to the ends of the test piece is negligible. As such the theoretical shape of a pinned-end column of length L_1, from x=0 to x=a remains an approximate straight line.

Thus again we see that in the case of pinned end practical columns even of lowest slenderness ratio that we tested the fact that "The swivelling blocks do not bend" does not affect the results for the buckling curve, calculated on the basis of distance between centres of balls being taken as true length of the column.

But any way the true "buckling stress Vs slenderness ratio" curve will lie below the one in which L_1 is representative in the expression for slenderness ratio and above the one in which 'L' is taken into account.

Therefore to this effect the buckling stress Vs L_1/K, curves have also been plotted in addition to the curves σ Vs L/K for M.S.round and rectangular section specimens pinned ends condition(see figures 5 and 6).

From these we note that the observed stress-slenderness ratio curve moves more nearer to the curves obtained by the available theories.

Thus in the end we conclude that there is definite close approximation between the theoretical and observed buckling curves for the M.S. and Al-Mg-alloy specimens of various compositions, and various sections, the samll deviations can be looked for by the safety factor.

4.6 c. EFFECT OF END-RESTRAINT

(i) M.S.round specimens.

Figure 10 shows the observed buckling curves for 7/16 in. round specimens (0.178%C) with fixed and pinned end conditions. Here two curves have been drawn for the pinned-ends condition. In one the slenderness ratio is based on the test piece length 'L' and in the other on the ~~test-p~~ distance between the centres of balls of the pinned end fixture.

Let us suppose that a design (utilising M.S.of the same composition as we have here i.e., 0.178%C) based on the pinned-ends condition has a working stress level of 47 K.S.i which is any arbitrary value chosen in the plastic range.

Then on the basis of curve No.3 figure 10 we see that at slenderness ratio of 64, we get the buckling stress of 47 K.S.i. But from the curve No.1 figure 10, we have at the slenderness ratio of 64, the buckling stress equal to 53.5 K.S.i. That is by constraining the ends from pinned to fixed ones we can raise the working stress for the same column from 47 K.S.i to 53.5 K.S.i(i.e., about 13.8% increase)[11] . It may be pointed out here that if we would have made calculations on the basis of curve No.2 figure 10, the working stress would have increased from 47 K.S.i to 60.25 K.S.i (i.e., about 28.2% increase). But as we have discussed above the more correct values are given by the curve No.3 in which the distance between the centres of balls is taken as the basis to calculate the slenderness ratio. Therefore we shall base our discussion on the values given by curve No.3 rather than curve No.2. That is a 13.8% increase in working stress is obtained in assumed working stress of 47.0 K.S.i. by constraining the ends from pinned to fixed .

On the other hand if the design is based on the fixed ends condition and the working range of slenderness ratio is pretty high, then corresponding to the same stress level as before i.e., 47 K.S.i. we have from curve No.1 figure 10 the value of slenderness ratio as 117. But from

---

[11] The corresponding increase on the theoretical basis is calculated ahead in next paragraph.

curve No.3 figure 10 we have, at this slenderness ratio of ~~120~~ 117, the stress equal to 34 K.S.i. Therefore in case we are somehow unable to incorporate the required fixed end conditions, the working stress level of the same column will fall from 47 K.S.i. to 34 K.S.i(i.e., about 28% reduction in value)*. This is a very high percentage of reduction in working stress of the column. As such it might lead to a dangerous state of affairs.

Therefore we conclude that for plastic designs i.e., designing for buckling on low slenderness ratios, it is advisible to design on the assumption of pinned-ends condition because even if in practice the pinned ends condition is not fulfilled, and which exactly happens, the design will tend to be more safe due to the rise in the working stress level. This rise in working stress level will not be 13.8% as anticipated above because the end conditions, if they are not pinned one, will never be fixed also. So the percentage rise in working stress level will not be too high either. Therefore the design, done on the pinned-ends condition will tend to be safer on one hand but not levish on the other. Secondly if the design would have been done on the basis of fixed-end conditions, we will definitely be on the dangerous side as the percentage reduction in the working stress level, which is pretty high may overtake the safety margin kept in design and the design might not work.

---

* The corresponding reduction on the theoretical basis is calculated ahead in the next paragraph.

Thus an excess of actual fixity over the assumed value can do little good but a lack of fixity under the assumed value can do much harm. Therefore as such conservatism should be used in selecting the fixity coefficient (Ref.equation 7) for use in plastic design.

Thirdly in the elastic range i.e., for values of slenderness ratio sufficiently high the value of 'C' in equn.(7) for fixed ends as '4' derived on the basis of Euler's theory, is never reached; e.g., at L/K=116,C=47/34=1.385. The reason which may be attributed to this is that a fixed-ends condition is not fully achieved due to some slip and similarly pinned-ends condition is not fulfilled due to friction at balls and the mating conical surfaces. Therefore the fixed-ends condition curve slightly shifts downwards and the pinned-ends condition curve moves little upward. The net effect of this is the reduction of the value of fixity coefficient of equation No.(7) and practically never equal to 4.

(ii) Effect of end-restraints on M.S(0.178%C) round specimens on basis of theoretical considerations.

Firstly let us assume that the design is done on the basis of pinned ends condition. Then assuming the same working stress level as before i.e., 47 K.S.i., from figure No.15, we have the value of $E_t = 29.4 \times 10^6$ p.s.i. Therefore the value of the slenderness ratio on the basis of tangent modulus theory is calculated as

$$(L/K)^2 = \frac{\pi^2 E_t}{\sigma_t}$$

$$= \frac{\pi^2 \times 29.4 \times 10^6}{47000} = 6200$$

$$\therefore \quad L/K = 78.6$$

Now supposing for the same test specimen the end restraints are made fixed ones. That is now we are to find the buckling stress for the fixed-ends condition with slenderness ratio as 78.6 and based on the tangent modulus theory.

This will have to be done by hit and trial since the tangent modulus is changing with stress and the stress value itself is not known.

Now for the fixed ends $\sigma_t = \frac{4\pi^2 E_t}{(L/K)^2}$

i.e., $\sigma_t = \frac{4\pi^2 E_t}{(78.6)^2}$ .....(23)

Assuming σ_t = 49.5 K.S.i, then from fig.15 $E_t = 7 \times 10^6$ p.s.i.

Then the right hand side of eqn. 23 reduces

to = $\frac{4\pi^2 \times 7 \times 10^6}{(78.6)^2}$ = 49450 p.s.i. = 49.45 K.S.i.

which is very near to 49.5 K.S.i.

Thus for the fixed ends, on the basis of tangent modulus theory the buckling stress corresponding to the slenderness ratio of 78.6 is 49.5 K.S.i.

Therefore the end restraints when changed from pinned to fixed ones increase the working stress level from 47 K.S.i to 49.5 K.S.i.

i.e., percentage increase in working stress

$$= \frac{2.5}{47} \times 100$$

$$= 5.3\%$$

as against the 13.8% rise obtained on the experimental basis.

Secondly let us assume that the design has been done on the basis of fixed-ends condition. Then assuming the same working stress as before i.e., 47 K.S.i.

From figure No.15 the value of $E_t = 29.4 \times 10^6$ p.s.i., and the value of the slenderness ratio on the basis of tangent-modulus theory is

$$(L/K)^2 = \frac{4\pi^2 E_t}{\sigma t}$$

$$= \frac{4\pi^2 \times 29.4 \times 10^6}{47000} = 24800$$

i.e., $L/K = 157.2$

Now supposing the fixed-ends condition is not fulfilled in practice but in the limiting case the ends are pinned ones. Then for the same slenderness ratio as above i.e., 157.2, the buckling stress can be formed by hit and trial as done below

$$\sigma t = \frac{\pi^2 E_t}{(L/K)^2}$$

$$\text{or} \quad \sigma t = \frac{\pi^2 \times E_t}{(157.2)^2} \qquad \ldots\ldots\ldots\ldots\ldots(24)$$

Assuming $\sigma t = 11.9$ K.S.i.

Then from figure 15, $E_t = 29.4 \times 10^6$ p.s.i.

Now right hand side of eqn. (24)

$$= \frac{\pi^2 \times 29.4 \times 10^6}{(157.2)^2} = 11880 \text{ p.s.i.}$$

$$= 11.88 \text{ K.S.i which is very near to assumed value of stress.}$$

Therefore due to the nonfulfilment of the fixed ends condition the working stress falls from 47 K.S.i to 11.9 K.S.i. (i.e., 75% reduction) for pinned ends.

The reason for the variation between the theoretical and the practical values of the percentage increase or decrease of the working stress owing to the non fulfilment of the end

conditions, may be that in practice the value of the fixity coefficient 'C' (Used in equation No.7) is never attained as '4' for the fixed ends. Thus the percentage reduction the working stress at the same slenderness ratio for the change of end conditions from fixed to pinned ones, will be less than 75% as obtained on the theoretical considerations. On the other hand the percentage increase in working stress at the same slenderness ratio for the change of end conditions from pinned to fixed ones is coming to be more in practical case than the theoretical one. The fact that the fixity coefficient is always less than '4' in practical columns suggests that there should be smaller increase in working stress in the practical case than the theoretical one. The reason for this may be that the bending moment on the pinned-end columns due to the manufacturing tolerances might be compratively more than the fixed-end columns, resulting in the relatively greater movement in the downward direction of the pinned-ends buckling curve, thereby increasing the distance between the two curves drawn on the same graph paper. That is the effective value of the percentage increase in working stress in the practical case may be even more than the one got on theoretical basis.

(iv) Effect of end restraints on At.Mg alloy (0.755% Mg.) round specimens. Fig. 11.

Fig. 11 shows the observed buckling curves for 7/16 in. dia. round specimens of At.Mg. alloy (0.755% Mg.) with fixed and pinned-ends conditions, drawn on the test piece length as basis for slenderness ratio calculations.

These curves show a marked inference that in the plastic range i.e. for low values of slenderness ratio the curves are very close to each other thereby reducing the end-restraint effect to a very low value. In fact what we observe is that the pinned-end curve is slightly higher than the fixed end curve. Firstly it may be due to some slip in the so called fixed ends causing the fixed-ends curve to move down slightly. Secondly the most prominent effect may be due to the slightly deformed conical cavities of the swivelling and the end blocks (this series of tests was performed last of all) of the rounded-ends fixture, and these defaced conical cavities would have increased the friction thereby giving fixing moments at the ends and thus giving higher buckling loads than the actual ones. That is the pinned end curve might have moved upwards rather to a greater extent. Secondly for a working stress of 28 K.S.I. (i.e. for higher slenderness ratio (107)) from the fixed end curve of Fig. 11 if the end restraints fail to be fixed ones but become pinned then the stress reduces from 28 to 19.2 K.S.I. i.e. 31.4% reduction.

(v) Effect of end-restraints on At.Mg. alloy (0.755% Mg.) round specimens on the basis of theoretical considerations.

First let us assume that the design is done on the basis of pinned-ends condition. Then assuming the working stress level, some where in plastic range say 36 K.S.I., we have from figure No.17 the corresponding value of tangent modulus $E_t = 3.45 \times 10^6$ P.S.I.

Therefore the value of the slenderness ratio on the basis of tangent modulus theory is calculated as

$$\left(\frac{L}{K}\right)^2 = \frac{\pi^2 E_t}{\sigma_t}$$

$$= \frac{\pi^2 \times 3.45 \times 10^6}{36000} = 9.47 \times 10^2$$

i.e. $\frac{L}{K} = 30.75$

Now supposing for the same test piece the end restraints are made fixed ones. That is now we are to find the buckling stress for the fixed ends condition with slenderness ratio as 30.75 and based on the tangent modulus theory.

This will have to be done by hit and trial since the tangent modulus is changing with the change in stress and the stress value itself is not known.

Now for the fixed ends

$$\sigma_t = \frac{4\pi^2 E_t}{(L/K)^2}$$

$$\text{i.e. } \sigma_t = \frac{4\pi^2 \times E_t}{(30.75)^2} \qquad \ldots\ldots\ldots\ldots\ldots\ldots \quad (25)$$

Assuming σ_t = 40.4 K.S.I., then corresponding value, from Fig. 17, of $E_t = 0.965 \times 10^6$ P.S.I.

Then the right hand side of equation No.25 reduced to

$$= \frac{4\pi^2 \times 0.965 \times 10^6}{(30.75)^2}$$

$$= 40.41 \text{ K.S.I.}$$

which is practically same as the assumed one i.e. 40.4. Thus for the fixed ends, on the basis of tangent modulus theory the buckling stress corresponding to the slenderness ratio of 30.75 is 40.4 K.S.I.

Therefore the end restraints when changed from pinned to fixed ones increase the working stress level from 36 K.S.I. to 40.4 K.S.I. i.e. percentage increase in working stress

$$= \frac{4.4}{36} \times 100 = 12.2\%$$

as against zero percent rise obtained on the experimental basis from the curves of Fig. 11. The reason, as explained earlier, may be due to the excessive friction at balls caused by the defaced conical cavities, which will shift the pinned-end curve upwards, thereby giving practically no percentage increase in working stress. Secondly let us assume that the design has been made on the basis of fixed-ends condition. Then assuming the working stress as 28 K.S.I. (i.e. for the higher slenderness ratio range), from the table No.17 the corresponding value of $E_t = 10.7 \times 10^6$ P.S.I. The value of the slenderness ratio on the basis of tangent modulus theory is

$$\left(\frac{L}{K}\right)^2 = \frac{4\pi^2 E_t}{\sigma_t}$$

$$= 4\,\frac{\pi^2 \times 10.7 \times 10^6}{28000} = 1.51 \times 10^4$$

i.e. $\frac{L}{K} = 123.$

Now supposing the fixed-ends condition is not fulfilled in practice but in the limiting case the ends are pinned ones. Then for the same slenderness ratio as above i.e. 123, the buckling stress can be found by bit and trial as below

$$\sigma_t = \frac{\pi^2 E_t}{(L/K)^2}$$

$$\text{or } \sigma_t = \frac{\pi^2 \times E_t}{(123)^2} \quad \ldots\ldots\ldots\ldots\ldots\ldots (26)$$

Assuming σ_t = 7 K.S.I., the corresponding value of E_t from Fig. 17 is 10.7×10^6 P.S.I. The right hand side of equation (26), then reduces to

$$\frac{\pi^2 \times 10.7\ 10^6}{(123)2} = 7000 \text{ P.S.I.}$$

which is same as the assumed one.

Therefore due to the nonfulfilment of fixed ends condition the working stress falls from 28 K.S.I. to 7 K.S.I. (i.e. 75% reduction) for pinned-ends as against the 31.4% reduction the practical columns.

The reason for the variation between the theoretical and practical values of the percentage decrease of working stress (for the higher slenderness ratio range) owing to the non-fulfilment of the fixed-ends condition, may be that in practice the value of the fixity coefficient 'C' (used in equation No.7) is never attained as '4' for the fixed ends. Thus the percentage reduction in working stress at the same slenderness ratio for the change of end

conditions from fixed to pinned will be less than 75% as obtained on the theoretical considerations. Also the upward shift of the observed pinned ends condition buckling curve, as explained above, tends to reduce this percentage reduction in working stress, still further. Thus we are in a position to conclude that the net practical percentage reduction in working stress (for the higher slenderness ratio range), if the fixed-ends condition fails to prevail and pinned-ends condition follows, will be much below the value as calculated theoretically.

5. CONCLUSIONS

1. Within the practical limitations there is close approximation between the theoretical and the observed data for the plastic range buckling of M.S. (.178% Carbon and .485% Carbon) and AL-Mg alloys (.755% Mg and .808% Mg) columns with various sections and end conditions.

2. For the buckling stresses in plastic region and near the stresses given by the knee of the compressive stress-strain curve of the material, the buckling seems to be governed by the tangent modulus theory, which dictates to simply replace the youngs modulus in the Eulers' expression for buckling by the tangent modulus of the material.

3. For the buckling stresses in the plastic region and far off the stresses given by the knee of the compressive stress-strain curve of the material, the buckling seems to be governed by the reduced modulus theory, which means simply to replace the youngs modulus in the Eulers' expression for buckling by the reduced modulus of the material.

4. In plastic range the effects of the end constraints tend to be negligible but with whatsoever is left conservatism should be used in selecting the fixity coefficient.

6. SUMMARY

Columns of M.S. (0.178% Carbon and 0.485% Carbon) and Al-Mg alloy (0.755% Mg and 0.808% Mg) of different sections (MS - round and rectangular; AL Mg alloy round and square) and different slenderness ratios were tested for buckling with pinned and fixed-ends conditions. The buckling stress Vs slenderness ratio curves so obtained were compared with the ones drawn on the basis of tangent and reduced modulii theories which were derived from the compressive stress-straincurves for the different materials. Close approximation between the theoretical and the observed practical curves was established. Whatsoever small deviations were there they could be explained on the basis of the non-fulfilment of the concentricity condition as well as the prescribed end-conditions. As such the effect in design of the nonfulfilment of the end conditions as well as that of the little eccentricity due to manufacturing tolerances could be taken care of by allowing safety factor.

In the plastic range the effects of the end constraints tend to be negligible and whatsoever is left should be dealt with by selecting the fixity coefficient with conservatism.

7. APPENDICES

(i) Table No.19

Calibration curve for 5-ton scale (Fig. 13)

Sr. No.	Corrected Machine Reading Tons	(Observed deflection of proving ring) $x10^4$ Inches	Sr. No.	Corrected Machine Reading Tons	(Observed deflection of proving ring) $x 10^4$ Inches
1.	0.000	0.0	11.	1.855	432.0
2.	0.055	15.0	12.	2.055	477.5
3.	0.255	61.0	13.	2.255	524.13
4.	0.455	108.6	14.	2.455	571.3
5.	0.655	156.0	15.	2.655	621.7
6.	0.855	201.3	16.	2.855	668.0
7.	1.055	246.16	17.	3.055	714.3
8.	1.255	291.1	18.	3.255	760.15
9.	1.455	338.6	19.	3.455	805.7
10.	1.655	385.16	20.	3.607	838.5

This curve along with the values in Table 20, has been plotted in Fig. 13 and with the help of these two curves the actual calibration curve for the 5-ton scale of the machine has been derived directly on the graph and shown in Fig. 12.

(ii) Table No.20

Proving ring curve (10,000 lb. capacity) (Fig.13)

Sr.No.	Load in lbs.	Deflection $x10^4$ Inches	Sr.No.	Load in lbs.	Deflection $x 10^4$ Inches
1.	2.	3.	1.	2.	3.
1.	500	41.0	7.	5000	413.6
2.	1000	82.4	8.	6000	497.8

Contd....

1.	2.	3.	1.	2.	3.
3.	1500	123.7	9.	7000	581.0
4.	2000	164.2	10.	8000	665.4
5.	3000	248.2	11.	9000	751.5
6.	4000	330.6	12.	10000	836.7

(iii) Table No.21

Calibration curve for 20-ton scale (Calibrated upto 10-tons only) (Fig. 14)

Sr. No.	Corrected Machine reading in Tons	Observed deflection of proving ring x 10^4 Inches.	Sr. No.	Corrected Machine reading in Tons.	Observed deflection of proving ring x 10^4 Inches.
1.	2.	3.	1.	2.	3.
1.	0.00	0.0	24.	4.43	472.0
2.	0.03	4.0	25.	4.63	491.0
3.	0.23	25.0	26.	4.83	512.0
4.	0.43	45.3	27.	5.03	531.6
5.	0.63	67.0	28.	5.23	552.16
6.	0.83	89.0	29.	5.43	572.0
7.	1.03	110.0	30.	5.63	592.3
8.	1.23	132.5	31.	5.83	613.0
9.	1.43	153.0	32.	6.03	633.3
10.	1.63	175.8	33.	6.23	652.2
11.	1.83	197.6	34.	6.43	673.0
12.	2.03	222.0	35.	6.63	692.5
13.	2.23	242.6	36.	6.83	713.3
14.	2.43	264.0	37.	7.03	733.0
15.	2.63	285.0	38.	7.23	753.9

Contd

1.	2.	3.	1.	2.	3.
16.	2.83	307.1	39.	7.43	775.0
17.	3.03	328.0	40.	7.63	796.0
18.	3.23	349.8	41.	7.83	817.3
19.	3.43	370.3	42.	8.03	838.2
20.	3.63	391.3	43.	8.23	859.0
21.	3.83	411.0	44.	8.43	880.0
22.	4.03	431.6	45.	8.63	900.0
23.	4.23	451.36			

1. The calibration of 20-ton scale has been done only upto 10-ton load due to the non availability of a proving ring beyond 10-ton capacity. Moreover we were to load the actual specimens only upto 9-tons maximum.

2. This curve alongwith the curve, tabulated in table No.22, has been plotted in Fig. 14, and with the help of these curves the actual calibration curve for 20-ton scale upto 10-tons load reading has been derived directly on the graph and shown in Fig. 14.

(iv) Table No.22

Proving ring curve (10-ton capacity) Fig. 14

Sr. No.	Load in tons	Deflection x 10^4 In.	Sr. No.	Load in tons.	Deflection x 10^4 In.
1.	2.	3.	1.	2.	3.
1.	0.5	54	11.	5.5	572
2.	1.0	106	12.	6.0	622
3.	1.5	158	13.	6.5	672
4.	2.0	212	14.	7.0	723

1.	2.	3.	1.	2.	3.
5.	2.5	266	15.	7.5	775
6.	3.0	318	16.	8.0	826
7.	3.5	369	17.	8.5	877
8.	4.0	420	18.	9.0	929
9.	4.5	471	19.	9.5	981
10.	5.0	522	20.	10.0	1032

(v) Table No.23

Compression test of M.S. (0.178% Carbon) Fig.15

Mean Dia of test specimen = 0.4541 In.

Length of test specimen = 0.8710 In.

The test was performed on 20-ton scale.

Sr. No.	Observed load Tons.	Deformation x 10^4 In.	Actual load from calibration curve Fig. 14 Tons.	Stress K.S.I.	Strain x 10^4 In./In.
1.	2.	3.	4.	5.	6.
1.	0.00	0.00	0.00	0.00	0.00
2.	0.45	1.00	0.45	6.22	1.15
3.	0.65	2.00	0.65	8.89	2.30
4.	0.85	5.00	0.85	11.75	5.74
5.	1.05	6.60	1.05	14.50	7.50
6.	1.25	6.61	1.25	17.30	7.50
7.	1.45	9.00	1.45	20.00	10.00
8.	1.85	9.20	1.85	25.60	10.00
9.	2.25	13.00	2.25	31.10	14.90
10.	2.45	13.10	2.45	33.90	14.95

Contd ....

1.	2.	3.	4.	5.	6.
11.	2.65	13.30	2.65	36.70	15.00
12.	2.85	13.95	2.85	39.40	16.00
13.	3.22	17.45	3.22	44.50	20.00
14.	3.32	18.30	3.32	47.00	21.00
15.	3.66	21.85	3.66	50.60	25.00
16.	3.76	48.00	3.76	52.00	55.00
17.	3.80	130.00	3.80	52.50	150.00
18.	4.02	221.00	4.02	55.50	255.00
19.	4.28	247.00	4.28	59.1	284.00
20.	4.48	292.00	4.48	62.0	336.00
21.	4.65	327.00	4.68	64.6	376.00
22.	4.85	368.00	4.90	67.8	424.00
23.	5.05	417.00	5.08	70.2	480.00
24.	5.25	463.00	5.30	73.3	531.00
25.	5.45	530.00	5.50	76.0	609.00
26.	5.65	600.00	5.70	78.8	690.00
27.	5.87	694.00	5.90	81.5	797.00
28.	6.05	772.00	6.10	84.3	886.00
29.	6.25	853.00	6.30	87.0	980.00
30.	6.45	980.00	6.50	89.8	1125.00
31.	6.65	1135.00	6.70	92.6	1190.0
32.	6.85	1210.00	6.90	95.4	1390.0
33.	7.05	1280.00	7.10	98.1	1470.0

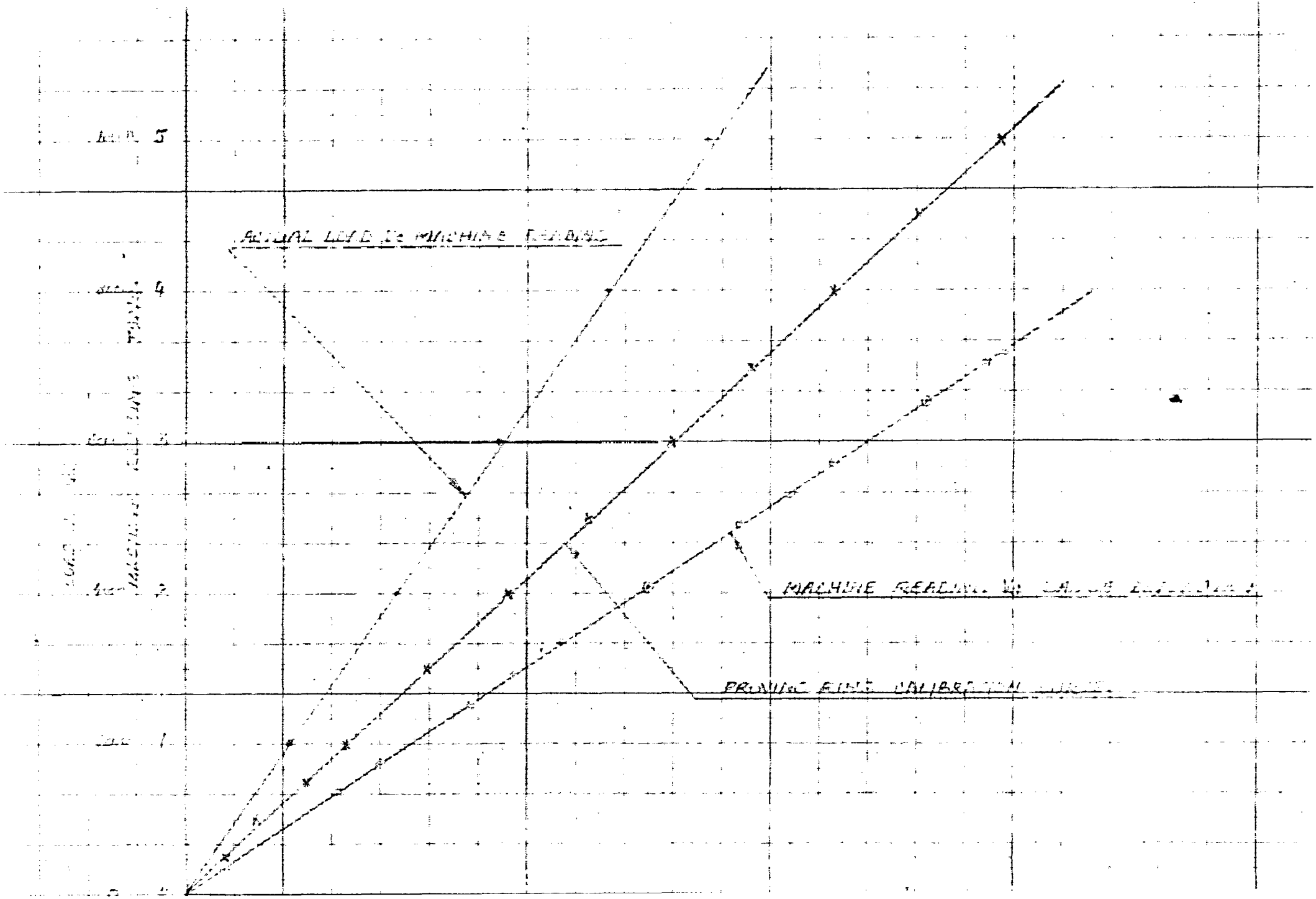
5
4
ACTUAL LOAD ON MACHINE FRAME
MACHINE READING
PROVING RING CALIBRATION

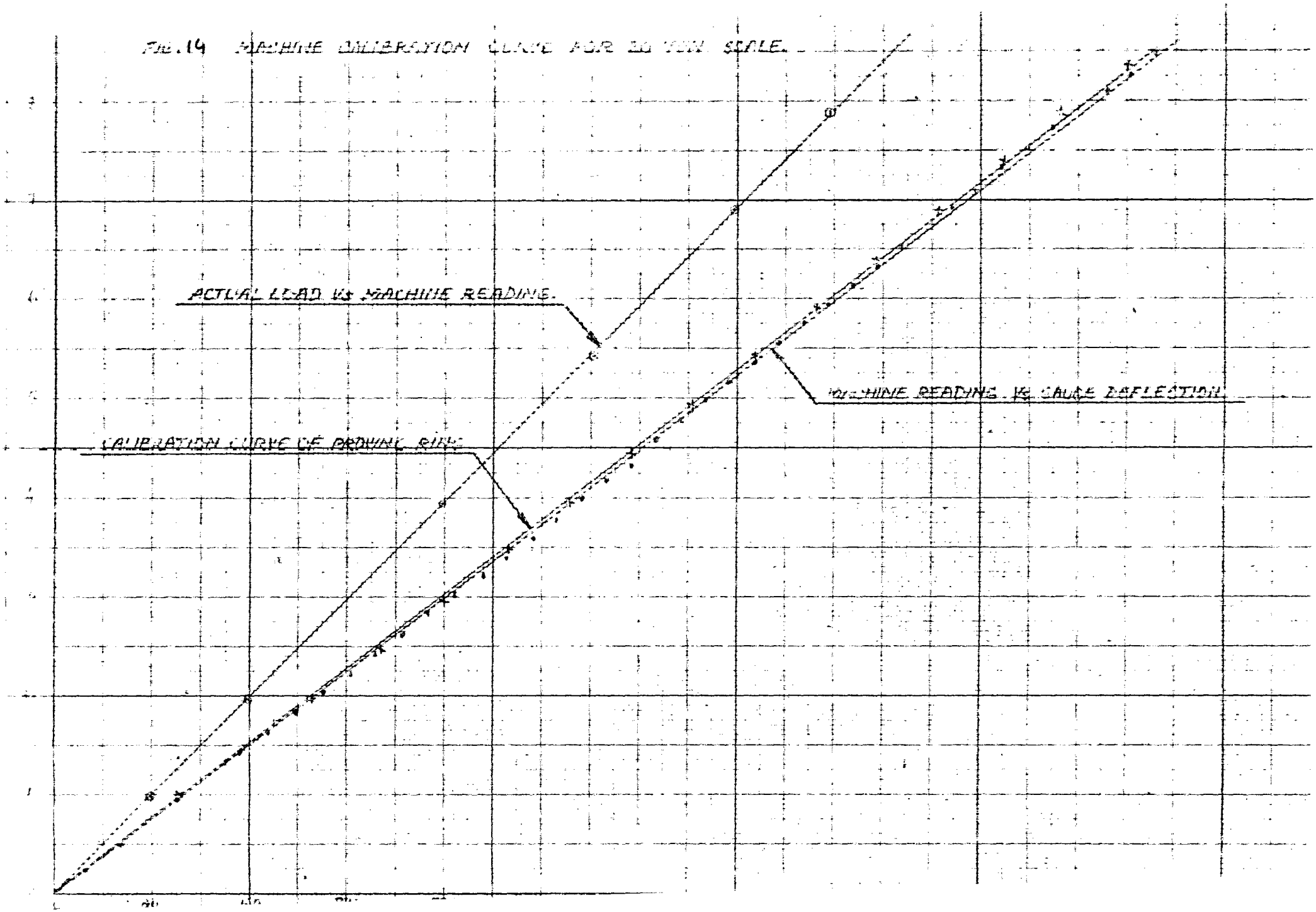
FIG. 14 MACHINE CALIBRATION CURVE FOR 20 TON SCALE
ACTUAL LOAD Vs MACHINE READING.
MACHINE READING Vs GAUGE DEFLECTION
CALIBRATION CURVE OF PROVING RING

(vi) Table No.24

Compression test of M.S. (0.485% Carbon) Fig. 16

Mean dia of test specimen = 0.4433 In.

Length of test specimen = 0.8854 In.

The test was performed on 20-ton scale.

Sr. No.	Observed load Tons.	Deformation x 10^4 In.	Actual load from Fig. 14. Tons	Stress K.S.I.	Strain x 10^4 In/In.
1.	2.	3.	4.	5.	6.
1.	0.00	0.00	0.00	0.00	0.00
2.	0.23	2.20	0.23	3.34	2.48
3.	0.43	3.98	0.43	6.24	4.50
4.	0.63	4.43	0.63	9.14	5.00
5.	0.85	4.44	0.85	12.60	5.00
6.	1.03	5.31	1.03	15.00	6.00
7.	1.23	5.40	1.23	17.85	6.10
8.	1.43	6.65	1.43	20.80	7.50
9.	1.63	7.09	1.63	23.70	8.00
10.	1.83	7.95	1.83	26.60	9.00
11.	2.03	8.85	2.03	29.50	10.00
12.	2.23	9.75	2.23	32.40	11.00
13.	2.43	10.62	2.43	35.20	12.00
14.	2.83	11.50	2.83	41.00	13.00
15.	3.03	13.30	3.03	44.00	15.00
16.	3.23	13.50	3.23	47.00	15.20
17.	3.43	14.60	3.43	49.70	16.50
18.	3.63	15.90	3.63	52.60	18.00
19.	3.83	16.10	3.83	55.00	18.20
20.	4.03	17.30	4.05	58.60	19.50

1.	2.	3.	4.	5.	6.
21.	4.23	23.90	4.25	61.60	27.00
22.	4.43	26.60	4.45	64.60	30.00
23.	4.63	52.30	4.65	67.50	59.00
24.	4.83	87.70	4.85	70.40	99.00
25.	5.03	106.20	5.06	73.40	120.00
26.	5.43	135.00	5.46	79.20	153.00
27.	5.83	159.00	5.86	85.00	180.00
28.	6.03	185.00	6.06	87.90	209.00
29.	6.23	203.00	6.28	91.10	229.00
30.	6.43	221.00	6.48	94.00	249.00
32.	6.63	242.00	6.68	97.00	273.00
33.	6.83	263.00	6.88	100.00	297.00
34.	7.03	282.00	7.08	103.00	318.00
35.	7.23	306.00	7.28	106.00	345.00
36.	7.43	330.0	7.48	108.50	372.00

(vii) Table No.25

Compressive Test of AL-Mg. alloy (0.755% Mg.) Fig.17

Mean dia of test specimen = 0.4360 In.

Length of test specimen = 0.8830 In.

The test was performed on 5-ton Scale.

Sr. No.	Observed load in Tons.	Deformation x 10^4 In.	Actual load from Fig. 13. Lbs.	Stress K.S.I.	Strain x 10^4 In./In.
1.	2.	3.	4.	5.	6.
1.	0.00	0.00	0.00	0.00	0.00
2.	0.43	5.30	900.0	6.00	6.00

Contd....

1.	2.	3.	4.	5.	6.
3.	0.80	7.05	1225	5.200	8.00
4.	0.90	8.38	1550	10.370	9.50
5.	1.00	10.60	1825	12.210	12.00
6.	1.10	12.35	2110	14.120	14.00
7.	1.20	12.36	2400	16.080	14.10
8.	1.30	13.25	2700	18.070	15.00
9.	1.50	17.65	3225	20.60	20.10
10.	1.70	22.9	3775	25.28	26.00
11.	1.80	23.8	4050	27.10	27.00
12.	2.00	26.5	4625	30.98	30.00
13.	2.05	28.2	4760	31.90	32.00
14.	2.20	31.8	5175	34.70	36.00
15.	2.30	34.80	5450	36.50	40.00
16.	2.40	38.7	5750	38.50	44.70
17.	2.45	42.0	5850	39.10	48.40
18.	2.50	46.7	6000	40.20	53.80
19.	2.55	54.0	6150	41.20	62.00
20.	2.60	63.5	6300	42.20	72.80
21.	2.65	85.0	6425	43.00	97.30
22.	2.70	111.5	6575	44.00	113.90
23.	2.75	137.5	6740	45.10	156.80
24.	2.80	164.5	6850	45.80	187.00
25.	2.85	190.0	6990	46.70	216.00
26.	2.90	222.0	7125	47.70	252.50
27.	2.95	252.0	7250	48.50	286.00
28.	3.00	288.0	7400	49.50	326.00
29.	3.10	374.0	7625	51.40	425.00

(viii) Table No.26

COMPRESSION TEST OF Al-Mg. ALLOY (0.808% Mg.) Fig. 18

Mean dia of test Specimen = 0.4526 In.

Length of test specimen = 0.8817 In.

The test was performed on 20-ton-scale

Sr. No.	Observed load Tons	Deformation x 10^4 In.	Actual load from Fig. 14. Tons	Stress K.S.I.	Strain x 10^4 In./In.
1.	2.	3.	4.	5.	6.
1.	0.00	0.00	0.00	0.00	0.0
2.	0.34	4.40	0.34	4.73	5.0
3.	0.54	5.30	0.54	7.50	6.00
4.	0.64	5.40	0.64	8.90	6.1
5.	0.74	7.05	0.74	10.30	8.0
6.	0.84	7.15	0.84	11.70	8.1
7.	1.04	13.20	1.04	14.50	15.0
8.	1.24	15.0	1.24	17.25	17.0
9.	1.44	17.6	1.44	20.00	20.00
10.	1.84	22.0	1.84	25.60	25.0
11.	2.24	25.5	2.24	31.20	30.0
12.	2.44	28.2	2.44	33.90	32.0
13.	2.64	35.3	2.64	36.70	40.0
14.	2.84	39.7	2.84	39.50	45.0
15.	3.04	63.5	3.04	42.3	72.0
16.	3.24	128.0	3.24	45.0	145.0
17.	3.44	309.0	3.44	47.8	350.0
18.	3.54	497.0	3.54	49.2	564.0
19.	3.64	724.0	3.64	50.0	800.0
20.	3.67	948.0	3.67	51.0	1075.0

(ix) Table No.27

Stress - Vs - Tangent modulus

curve for M.S. 0.178% Carbon (Fig. 15)

Sr. No.	Stress K.S.I.	Tangent modulus $E_t \times 10^{-6}$ P.S.I.	Sr. No.	Stress K.S.I.	Tangent modulus $E_t \times 10^{-6}$ P.S.I.
1.	0.0 to 48.0	29.4	6.	55.0	0.93
2.	48.5	17.7	7.	65.0	0.59
3.	50.0	6.6	8.	75.0	0.396
4.	51.0	3.6	9.	85.0	0.28
5.	52.0	2.0	10.	90.0	0.18

(x) Table No.28

Stress Vs Tangent modulus curve for

M.S. (0.485% Carbon) Fig. 16

Sr. No.	Stress K.S.I.	Tangent modulus $E_t \times 10^{-6}$ P.S.I.	Sr. No.	Stress K.S.I.	Tangent modulus $E_t \times 10^{-6}$ P.S.I.
1.	0 to 55.00	30.00	7.	63.40	2.56
2.	55.10	27.30	8.	68.00	1.54
3.	55.50	20.20	9.	70.00	1.61
4.	56.15	14.20	10.	80.00	1.60
5.	58.00	9.40	11.	90.00	1.50
6.	60.50	5.51	12.	100.00	1.20

(xi) Table No.29

Stress Vs Tangent modulus curve for Al.Mg alloy (0.755% Mg) Fig. 17.

Sr. No.	Stress K.S.I.	Tangent modulus $E_t \times 10^{-6}$ P.S.I.	Sr. No.	Stress K.S.I.	Tangent modulus $E_t \times 10^{-6}$ P.S.I.
1. 0 to	30.00	10.70	9.	39.60	1.60
2.	30.60	9.40	10.	41.75	0.95
3.	31.60	8.00	11.	42.60	0.65
4.	32.50	6.67	12.	43.30	0.47
5.	33.70	5.43	13.	44.00	0.35
6.	34.70	4.75	14.	45.50	0.26
7.	36.60	3.33	15.	46.00	0.20
8.	38.50	2.45			

(xii) Table No.30

Stress Vs Tangent modulus curve Al.Mg alloy (0.808% Mg) Fig. 18

Sr. No.	Stress Vs K.S.I.	Tangent modulus $E_t \times 10^{-6}$ P.S.I.	Sr. No.	Stress Vs K.S.I.	Tangent modulus $E_t \times 10^{-6}$ P.S.I.
1. 0 to	34.0	10.60	7.	43.0	0.74
2.	34.5	7.70	8.	44.0	0.48
3.	35.0	4.72	9.	45.0	0.24
4.	37.0	2.85	10.	46.0	0.18
5.	39.0	1.88	11.	48.0	0.08
6.	41.0	1.13	12.	50.0	0.04

FIG-15 CHARACTERISTIC CURVES OF M.S. CUT OF CIRCULAR BARS.

COMPOSITION:- 0.17 % CARBON

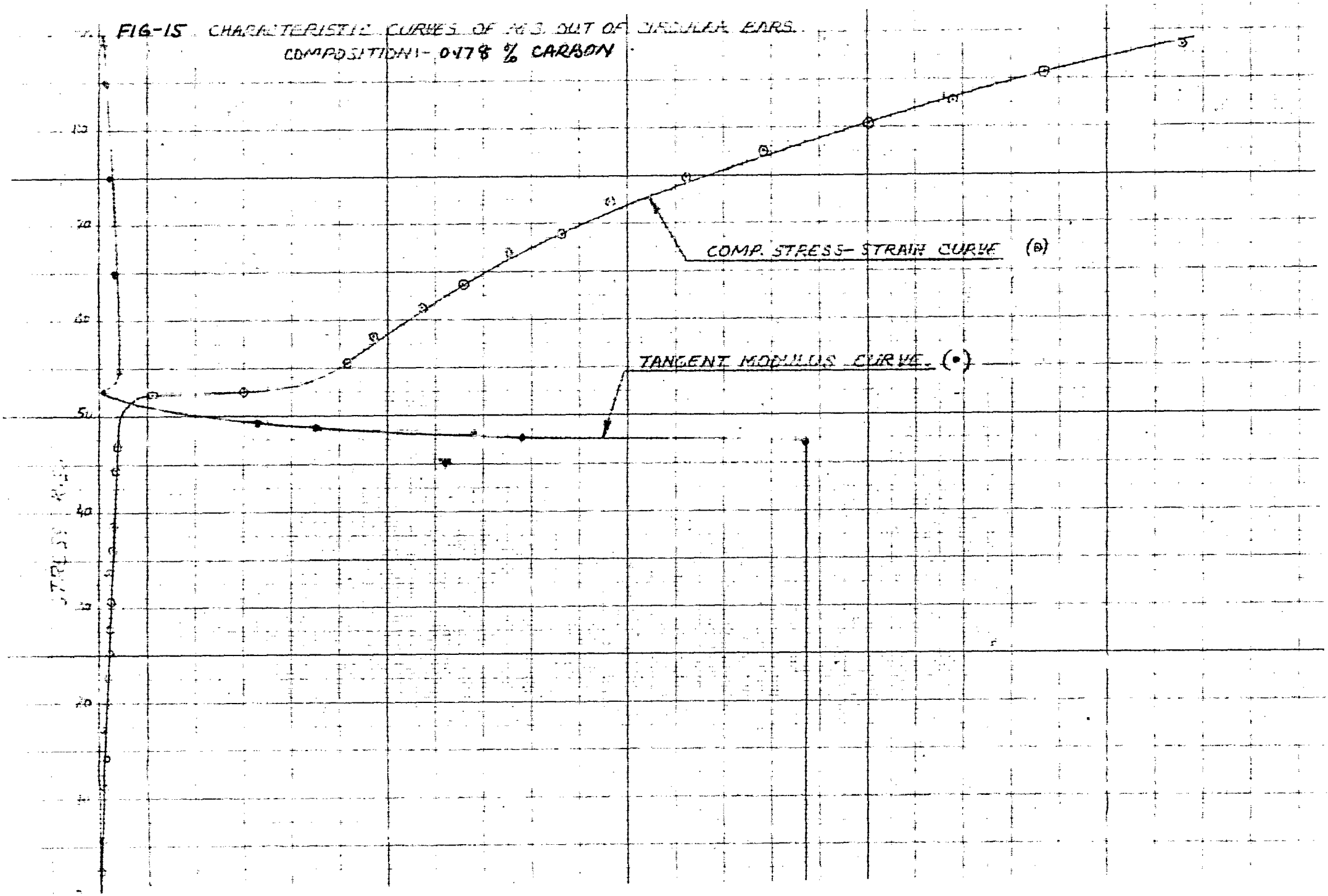

FIG-16 CHARACTERISTIC CURVES OF M.S. OUT OF RECTANGULAR BARS

COMPOSITION :- 0.485 % CARBON

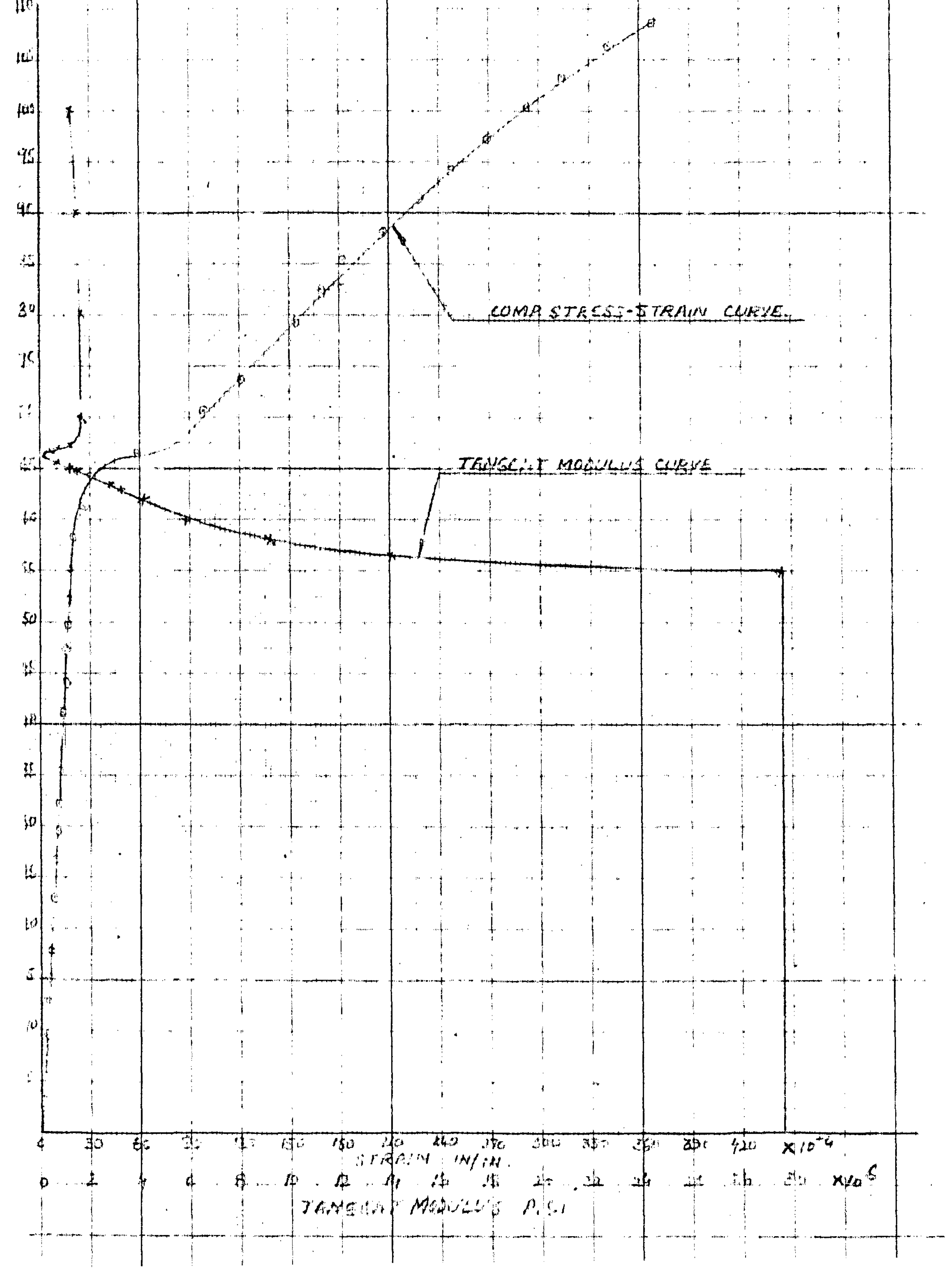

FIG-11 CHARACTERISTIC CURVES OF AlMg ALLOY CUT OF CIRCULAR BARS
COMPOSITION = 0.755 % Mg

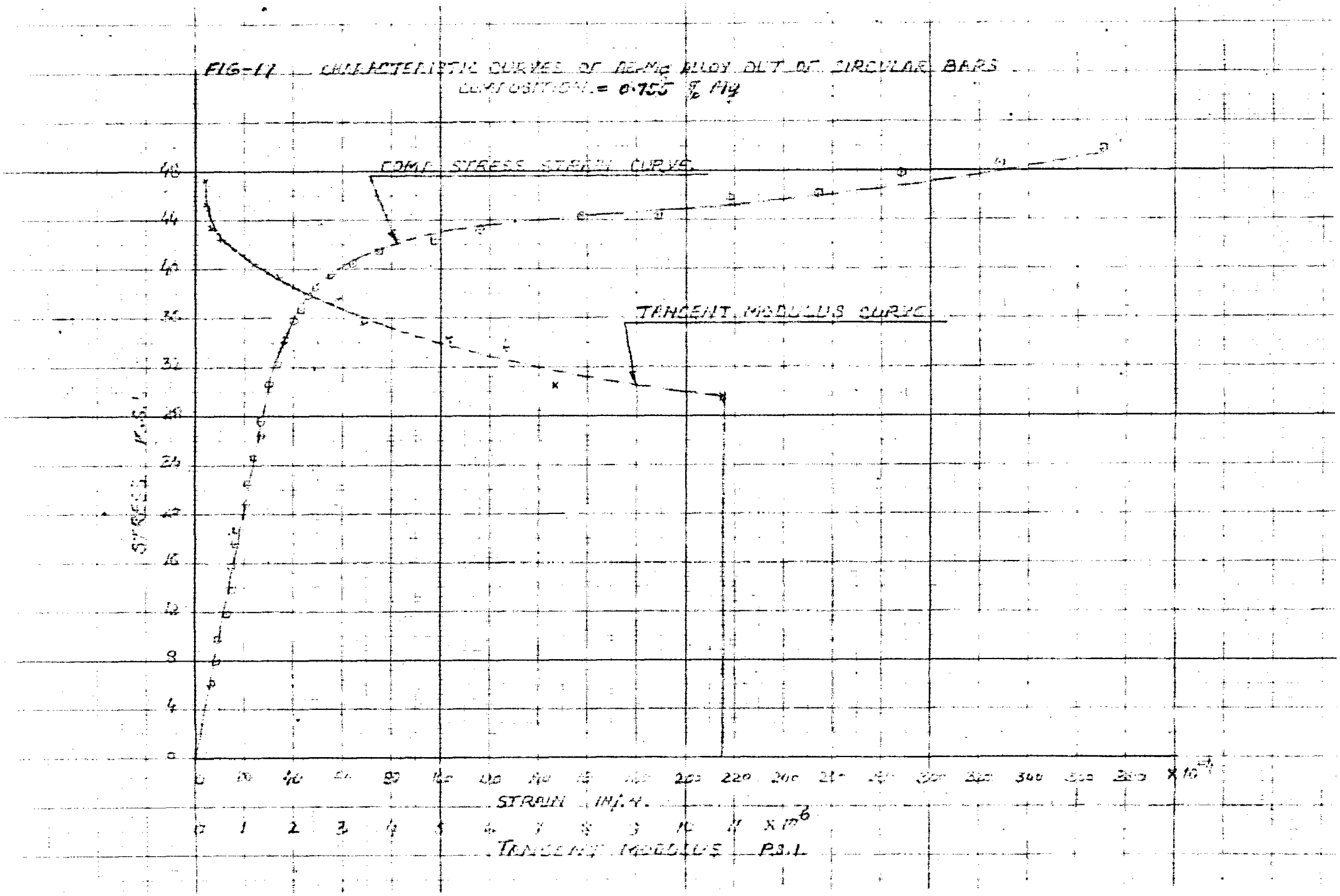

FIG-12 CHARACTERISTIC CURVES OF ALUMINIUM-MAGNESIUM ALLOY OUT OF SOLID BARS

COMPOSITION = 6.180% Mg.

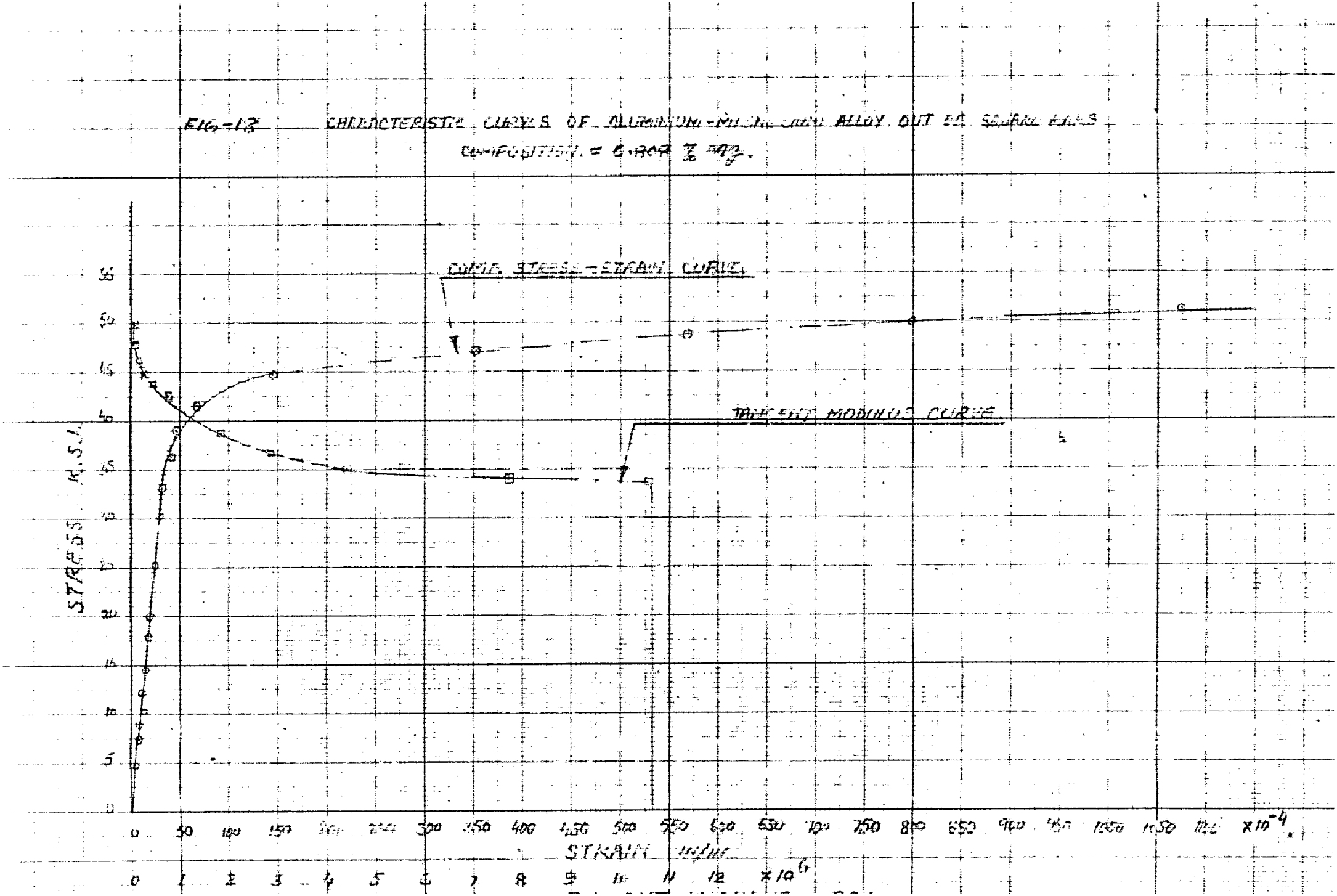

8. BIBLIOGRAPHY

1. Bleich, F: "Buckling strength of metal structures". McGraw-Hill book Company, Inc.,New York,1952.

2. Seely, Fred B. and Smith, James O: "Advanced Mechanics of Materials". John Wiley and Sons, Inc. New York, 1959.

3. Shanley, F.R: "Inelastic column Theory". J. Aeronaut. Sci, Vol. 13, No.12, December 1946.

4. Shanley, F.R: "Applied column Theory". Transactions of American Society of Civil Engineers Vol. 115, 1950 Page 698-727.

5. Duberg, J.E. and T.W. Wilder, III: "Inelastic column Theory". NACA TN 2267, Jan. 1951.

6. Shanley, F.R: "Strength of Materials". McGraw-Hill book Company, Inc, New York, 1957.

7. Von Kármán, Th., E.E. Sechler, and L.H. Donnell: "The strength of thin plates in compression". Trans. A.S.M.E., Vol. 54 No.2,June 30,1932.

8. Suresh Chandra and A.B.L. Aggarwal: "Laboratory Manual of Applied Instrumentation" Department of Mechanical Engineer, University of Roorkee, Roorkee, U.P., 1962.